



U.S. Department of
Transportation

**Federal Railroad
Administration**

Validating Electromagnetic Walking Stick Rail Surface Crack Measuring Systems

Office of Research,
Development,
and Technology
Washington, DC 20590



NOTICE

This document is disseminated under the sponsorship of the Department of Transportation in the interest of information exchange. The United States Government assumes no liability for its contents or use thereof.

NOTICE

The United States Government does not endorse products or manufacturers. Trade or manufacturers' names appear herein solely because they are considered essential to the objective of this report.

REPORT DOCUMENTATION PAGE			<i>Form Approved</i> OMB No. 0704-0188	
Public reporting burden for this collection of information is estimated to average 1 hour per response, including the time for reviewing instructions, searching existing data sources, gathering and maintaining the data needed, and completing and reviewing the collection of information. Send comments regarding this burden estimate or any other aspect of this collection of information, including suggestions for reducing this burden, to Washington Headquarters Services, Directorate for Information Operations and Reports, 1215 Jefferson Davis Highway, Suite 1204, Arlington, VA 22202-4302, and to the Office of Management and Budget, Paperwork Reduction Project (0704-0188), Washington, DC 20503.				
1. AGENCY USE ONLY (Leave blank)		2. REPORT DATE June 2016		3. REPORT TYPE AND DATES COVERED Technical Report
4. TITLE AND SUBTITLE Validation of Electromagnetic Walking Stick Rail Surface Crack Measuring Systems			5. FUNDING NUMBERS	
6. AUTHOR(S) and FRA COTR Eric Magel				
7. PERFORMING ORGANIZATION NAME(S) AND ADDRESS(ES) National Research Council, Canada 2320 Lester Road, Ottawa, Canada K1V 1S2			8. PERFORMING ORGANIZATION REPORT NUMBER AST-R-LR-0102	
9. SPONSORING/MONITORING AGENCY NAME(S) AND ADDRESS(ES) U.S. Department of Transportation Federal Railroad Administration Office of Research, Development, and Technology Washington, DC 20590			10. SPONSORING/MONITORING AGENCY REPORT NUMBER DOT/FRA/ORD-16/23	
11. SUPPLEMENTARY NOTES COTR: Ali Tajaddini, PE				
12a. DISTRIBUTION/AVAILABILITY STATEMENT This document is available to the public through the FRA web site at https://www.fra.dot.gov/eLib/Find or calling 202-493-1300			12b. DISTRIBUTION CODE	
13. ABSTRACT (Maximum 200 words) A series of field studies were undertaken to evaluate electromagnetic walking stick systems and their ability to measure the depth of damage from surface breaking cracks. In total, four railroads, and four suppliers participated in the project. The walking sticks were able to determine whether cracks are present and, after multiple runs, whether crack length is increasing or declining. None of the evaluated units were able to accurately quantify crack depth. While the crack depth predictions most often exceeded the "measured/real" values, sometimes by 200 or 300%, the systems can determine where along the track (and where across the railhead) that cracking is present. This information may be useful for planning of rail grinding, monitoring and trending the progress in reducing and eliminating cracks, identifying clusters of damage at high resolution and point to localized problems with track geometry or other errors. Lastly these tools could be used to qualitatively evaluate the effectiveness of, for example, friction management, improved profiles and steels in mitigating surface fatigue.				
14. SUBJECT TERMS			15. NUMBER OF PAGES 62	
			16. PRICE CODE	
17. SECURITY CLASSIFICATION OF REPORT Unclassified	18. SECURITY CLASSIFICATION OF THIS PAGE Unclassified	19. SECURITY CLASSIFICATION OF ABSTRACT Unclassified	20. LIMITATION OF ABSTRACT	

NSN 7540-01-280-5500

Standard Form 298 (Rev. 2-89)
Prescribed by ANSI Std. Z39-18
298-102

METRIC/ENGLISH CONVERSION FACTORS

ENGLISH TO METRIC

LENGTH (APPROXIMATE)

1 inch (in)	=	2.5 centimeters (cm)
1 foot (ft)	=	30 centimeters (cm)
1 yard (yd)	=	0.9 meter (m)
1 mile (mi)	=	1.6 kilometers (km)

AREA (APPROXIMATE)

1 square inch (sq in, in ²)	=	6.5 square centimeters (cm ²)
1 square foot (sq ft, ft ²)	=	0.09 square meter (m ²)
1 square yard (sq yd, yd ²)	=	0.8 square meter (m ²)
1 square mile (sq mi, mi ²)	=	2.6 square kilometers (km ²)
1 acre = 0.4 hectare (he)	=	4,000 square meters (m ²)

MASS - WEIGHT (APPROXIMATE)

1 ounce (oz)	=	28 grams (gm)
1 pound (lb)	=	0.45 kilogram (kg)
1 short ton = 2,000 pounds (lb)	=	0.9 tonne (t)

VOLUME (APPROXIMATE)

1 teaspoon (tsp)	=	5 milliliters (ml)
1 tablespoon (tbsp)	=	15 milliliters (ml)
1 fluid ounce (fl oz)	=	30 milliliters (ml)
1 cup (c)	=	0.24 liter (l)
1 pint (pt)	=	0.47 liter (l)
1 quart (qt)	=	0.96 liter (l)
1 gallon (gal)	=	3.8 liters (l)
1 cubic foot (cu ft, ft ³)	=	0.03 cubic meter (m ³)
1 cubic yard (cu yd, yd ³)	=	0.76 cubic meter (m ³)

TEMPERATURE (EXACT)

$$[(x-32)(5/9)]^{\circ}\text{F} = y^{\circ}\text{C}$$

METRIC TO ENGLISH

LENGTH (APPROXIMATE)

1 millimeter (mm)	=	0.04 inch (in)
1 centimeter (cm)	=	0.4 inch (in)
1 meter (m)	=	3.3 feet (ft)
1 meter (m)	=	1.1 yards (yd)
1 kilometer (km)	=	0.6 mile (mi)

AREA (APPROXIMATE)

1 square centimeter (cm ²)	=	0.16 square inch (sq in, in ²)
1 square meter (m ²)	=	1.2 square yards (sq yd, yd ²)
1 square kilometer (km ²)	=	0.4 square mile (sq mi, mi ²)
10,000 square meters (m ²)	=	1 hectare (ha) = 2.5 acres

MASS - WEIGHT (APPROXIMATE)

1 gram (gm)	=	0.036 ounce (oz)
1 kilogram (kg)	=	2.2 pounds (lb)
1 tonne (t)	=	1,000 kilograms (kg)
	=	1.1 short tons

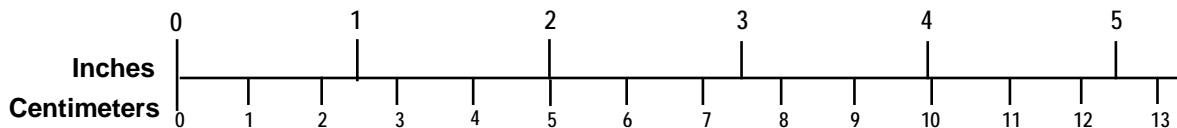
VOLUME (APPROXIMATE)

1 milliliter (ml)	=	0.03 fluid ounce (fl oz)
1 liter (l)	=	2.1 pints (pt)
1 liter (l)	=	1.06 quarts (qt)
1 liter (l)	=	0.26 gallon (gal)
1 cubic meter (m ³)	=	36 cubic feet (cu ft, ft ³)
1 cubic meter (m ³)	=	1.3 cubic yards (cu yd, yd ³)

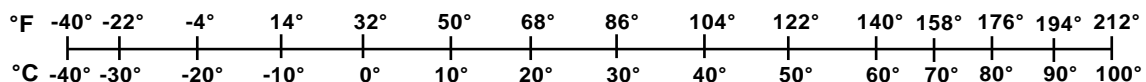
TEMPERATURE (EXACT)

$$[(9/5)y + 32]^{\circ}\text{C} = x^{\circ}\text{F}$$

QUICK INCH - CENTIMETER LENGTH CONVERSION



QUICK FAHRENHEIT - CELSIUS TEMPERATURE CONVERSION



For more exact and or other conversion factors, see NIST Miscellaneous Publication 286, Units of Weights and Measures. Price \$2.50 SD Catalog No. C13 10286

Updated 6/17/98

Contents

Executive Summary	7
1. Introduction	8
2. Objective.....	10
3. Activities.....	11
3.1 CSX Rail Samples – Measurements Versus Metallurgical Sectioning	11
3.2 Pre and Post-Grinding Measurements on CSX	15
3.3 NS Hardy Curve Samples.....	21
3.4 BNSF Staples Subdivision – measurements versus milling.....	24
3.5 A Transit Example.....	26
4. Conclusions	27
5. Acknowledgements	31
6. References	32
Appendix A Details of the Surface Crack Measuring Systems	33
Appendix B Validating Electromagnetic Surface Crack Measuring Systems	35
B.1 CSX rail samples from June 2013	35
B.2 NRC Sectioned CSX rail samples	36
B.2.1. Non-Destructive Testing (NDT) crack measurements of CSX rail samples.....	47
B.3 NS Railways samples from February 2014	50
B.3.1. NS metallurgical sectioning	50
B.3.2. NS milling	53
B.4 BNSF Rail Samples from November 2014	55
B.4.1. Sample 3	55
B.4.2. Sample 4	56
B.4.3. Sample 6	57
B.4.4. Sample 8	58
B.4.5. Sample 16	59
Abbreviations and Acronyms	60

Illustrations

Figure 1: The process followed for determining the depth of the surface cracks.....	12
Figure 2: The process to mill and chase cracks through the rail head.	13
Figure 3: Comparison of crack depth measurements obtained with the MRX and Rohmann systems with those obtained through destructive sectioning and milling. The milled samples (which should be the most reliable) are highlighted with the blue box.	15
Figure 4: Method for evaluating the depth of metal removed at each test site. This is a low/inside rail example.....	17
Figure 5: Example of RSCM data collected from the high rail of curve CA 551.65 which received six grinding passes.....	Error! Bookmark not defined.
Figure 6: Example of RSCM data showing crack depth measurements.....	19
Figure 7: Although the 4 probes on Rohmann’s Draisine can be repositioned, they are commonly left at a gauge corner position, even on low rail measurements.	20
Figure 8: Results of CSX rail grinding tests – metal removed by grinding is compared with the measured shortening of the cracks. The asterix denotes cases where the final crack depth was zero.	21
Figure 9: The Hardy curve on the Norfolk Southern Railways is 5.7°. The low rail was last ground June 2013 and the high rail on November 2013. The low rail was removed from service two weeks later and eight samples removed.	22
Figure 10: Two scans of the RSCM unit over the Hardy curve, with test site locations marked.	22
Figure 11: Sectioning of three rail samples and crack measurement were undertaken by NS Labs.	23
Figure 12: Summary of results for measurement versus machining of rail samples on NS Hardy curve.....	24
Figure 13: Layout of BNSF Staples samples for measurement with the walking sticks.....	25
Figure 14: Comparison of electromagnetic measurements with milling results.....	26
Figure 15: Difference between the pre- and post-grind rail profiles shows that 0.88 mm of metal was removed from the gauge corner.....	26
Figure 16: The progression of damage as measured with the MRX RSCM. The depth and extent of cracking is seen clearly to grow with time.	29
Figure 17: The three electromagnetic based systems evaluated through this program.	33
Figure 18: CSX Rail sample #2. Water jet cut perpendicular to surface cracks.....	36
Figure 19: CSX Rail sample #4. Water jet cut perpendicular to surface cracks with dry (red) magnetic particle enhancement of cracks.	37
Figure 20: CSX Rail sample #6. Water jet cut perpendicular to surface cracks with dry and liquid magnetic particle enhancement.	38

Figure 21: CSX Rail sample #6. Water jet cut along the length of the rail, liquid magnetic particle enhancement.	39
Figure 22: CSX Rail sample #7. Water jet cut perpendicular to surface cracks, dry (red) magnetic particle enhancement of cracks. And then milled down through top of rail in 0.4 mm increments.....	40
Figure 23: CSX Rail sample #12. Water jet cut perpendicular to surface cracks, and then along the length of the rail, dry (red) and liquid magnetic particle enhancement.	41
Figure 24: CSX Rail sample #14. Milled through the rail crown in 0.4 mm increments.	42
Figure 25: CSX Rail sample #16. Water jet cut perpendicular to surface cracks, dry (red) magnetic particle enhancement.....	43
Figure 26: CSX Rail sample #16. Water jet cut along the length of the rail, liquid magnetic particle enhancement.	44
Figure 27: CSX Rail sample #6. Water jet cut along the length of the rail, liquid magnetic particle enhancement.	45
Figure 28: CSX Rail sample #18. Water jet cut along the length of the rail, liquid magnetic particle enhancement.	46
Figure 29: NS Labs analysis of Sample 4.....	50
Figure 30: NS Labs analysis of Sample 5.....	51
Figure 31: NS Labs analysis of Sample 6, longitudinal section	52

Tables

Table 1: Summary of results for RSCM and Draisine measurements vs measured cracks depth through rail sectioning and milling	14
Table 2: Seven curves were measured on the CSX railroad before and after rail grinding.....	16
Table 3: Depth of metal removed by rail grinding.	18
Table 4: Comparison of features: MRX, Rohmann and Sperry walking stick devices	34

Executive Summary

Beginning in summer 2013, the capability of electromagnetic testing based walking stick instruments to detect and measure surface defects from Rolling Contact Fatigue (RCF), as they propagate into the rail, was evaluated via a series of field studies. These studies included field measurements of rail that belongs to CSX and Norfolk Southern (NS) Railways, and involved extensive metallurgical work to determine crack depths for comparison with the field measurements. The Rail Surface Crack Management (RSCM) unit from MRX Technologies and the Draisine unit from Rohmann GmbH (and later the Sperry unit), could determine whether cracks are present and whether crack length is increasing or declining.

However, the systems are not currently able to accurately quantify crack depth. The crack depth predictions often exceeded the “measured or real” values, sometimes by 200 or 300%. There is some evidence to suggest that measurements of crack length with Eddy Current are good but the translation to depth is fraught with difficulty, since the crack orientations and propagation angles have large variations in the North American freight context.

Accordingly, these magnetism-based tools can be used for:

- Determining whether and where measurable cracks are present.
- Identifying the location of surface fatigue on the railhead.
- Providing a relative assessment of the severity of cracking on the rail.

This information could be:

- Valuable for planning of rail grinding, especially when coupled with rail profiles. Concentrations of RCF at certain positions across the railhead can point to changes required in the rail profiles and grinding patterns.
- Used to monitor and trend the progress in reducing and eliminating cracks (similar to the Grinding Quality Index (GQI) that is used to monitor transverse rail profile deviations).
- Applied to identify clusters of damage at high resolution and point to localized problems with track geometry or other errors.
- Used qualitatively to investigate the effectiveness of, for example, friction management, improved profiles, and steels in mitigating surface fatigue.

The project participants agreed that a much larger number of measured and sectioned rails are needed to fully characterize the crack morphology under typical North American conditions and facilitate credible calibrations. This is especially true for the low rail, since all the units were initially developed with a focus on gauge corner cracking of the high rail and low rail. As a result, RCF on freight railroads is proving difficult to measure thus far.

1. Introduction

Rail surface fatigue is a natural result of the many loading cycles that the rail must bear from the passing wheelsets. It is the cumulative effect of high stress at the wheel-rail contact that causes plastic deformation and leads to calls for regular maintenance. It is important to monitor, identify and treat rolling contact fatigue (RCF) cracking, shelling and squats to maintain the safety and reliability of the rail.

The measurement of crack depth would normally require the removal of rail samples from the field, which are broken in the laboratory or otherwise sectioned for inspection. Fortunately, non-destructive tools that are reportedly capable of assessing crack depths are emerging. In a project undertaken in 2006 the National Research Council (NRC) in Canada evaluated four different eddy-current-based systems that claimed to be able to measure the pocket depth of surface cracks [1]. At the time, these systems proved inadequate when they were tested on several cracked rails collected from across North America. However development continued, especially in Germany. On German railways, eddy current walking sticks are used extensively and as of 2013, “all rail maintenance machines” are required to document with an eddy current machine the results of their operations on the extent of surface fatigue [2].

In North America, Loram Maintenance of Way, Inc. has acquired a system from MRX Technologies in Australia that uses the level of magnetic flux leakage to estimate the crack depth directly. Rohmann GmbH (based in Germany) has over the last several years continued to improve the capabilities of its eddy-current-based Draisine unit and has begun using it on select test locations in North America. Finally, Sperry Rail Services has introduced an eddy current based system, which is included in its multi-technology platform for complete rail inspection. Hy-rail based systems have arrived in North America and are now being tested in the field.



The MRX hy-rail RSCM unit



Rohmann's hy-rail eddy current unit can have as many as 6 probes per rail. Operating speeds are up to 40 mph.

In North America there are strong safety and economic interests in learning the rate of crack growth and the risks associated with cracking in the rail. Safety implications of RCF include more than 100 derailments reported by the Federal Railroad Administration (FRA) each year and compromised ultrasonic testing, while the cost of monitoring and treating rail for RCF problems

is significant. Rail replacement due to RCF costs over \$300 million annually, and additional costs come from inspection, derailments and damage to track and rolling stock components. Of the more than \$100 million dollars spent annually on rail grinding in North America, at least 30% can be attributed to RCF [3].

If instruments were able to reliably and accurately measure the depth of surface breaking cracks, they would eliminate the current need for destructive removal of rail samples, and would enable the rapid collection of crack depths for a range of applications, including studies of crack growth rates for various rail steels as well as environmental and operating conditions, risk assessment for cracked rail, and for developing improved grinding strategies.

There are three possible methods that could validate the accuracy of surface crack measuring systems.

1. Insert an artificial defect that has a known depth and orientation (e.g. a vertical crack using wire electrical discharge machining (EDM) or spark erosion) and compare it with the measured value. This is commonly done by the original equipment manufacturer (OEM) in a laboratory environment when developing the instruments and may be used on a regular basis later to recalibrate them. However, the morphology of cracks in the field requires that a validation include “real-world” conditions, including angle of crack propagation, shape into the rail, orientation with respect to the scanning trajectory of the instrument, and presence of other cracks and surface irregularities.
2. Measure cracks on a rail with visible surface fatigue, and then use a rail grinder to remove metal until the cracks just disappear. Determine whether the depth of metal removed corresponds with the measurement of crack depth. This approach was followed by Loram when trialing a prototype RSCM system. They were able to satisfy themselves that the unit was giving reliable measurements.
3. Measure cracks on a rail with visible surface fatigue and then remove a short length of rail. Section the rail sample and measure the crack length and depth into the rail.

Several studies using methods 2 and 3 were undertaken in this project and are the subject of this report.

2. Objective

To determine whether electromagnetic testing based walking stick instruments are able to reliably and accurately measure surface crack depths on steel rails.

3. Activities

Through a collaborative project, representatives from Loram, Rohmann, MRX, Sperry, NRC and the NS and CSX railways participated in a series of field measurements and metallurgical sectioning programs. Three different studies were undertaken to validate the Draisine and RSCM systems. Sperry joined the program in 2015 and participated in the fourth validation effort.

1. Thirty rail samples with differing levels of fatigue on different types of rail steel were measured, photographed and then removed from CSX track in the Bluefield Mountains of Tennessee. Twenty of these samples were shipped to NRC in Ottawa and eight of them were subjected to metallurgical sectioning. Three other samples were sent from Tennessee to MRX in Australia. The crack depths obtained through sectioning were compared with the Draisine/RSCM measurements.
2. Three days of pre- and post-grind measurements on CSX track in Kentucky. Seven curves were photographed and then measured for profile and crack depth, next the rail was ground with up to 6 passes by a large production grinder, and then the measurements and photographs were repeated. The change in measured crack depth was compared with the amount of metal removed through grinding.
3. Measurements of crack depth and photo-documentation were made at the Hardy curve (NS). At this curve, NS and Loram had previously established test locations that were being monitored with the Rohmann and MRX instruments. Eight test locations were marked for rail removal. These were then sectioned by the R&D group at NS to determine the actual crack depth, and those measurements then compared with the Rohmann/MRX measurements.
4. Fourteen rail samples were selected from rail relay sections on BNSF's Staples subdivision. These were shipped to Loram's technical center in Hamel, Minnesota and set end to end for subsequent scanning with the MRX, Rohmann and Sperry units. Also included for testing was a rail length from a switch where rail had fractured into several pieces to cause a derailment. Five rail samples were milled at the University of Alberta and crack mapping undertaken by NRC. The measured depths of cracking were compared with the MRX/Rohmann/Sperry measurements.
5. A comparison of field measurement of gauge corner cracking in Dubai with the amount of metal removed during grinding to address it was made.

3.1 CSX Rail Samples – Measurements Versus Metallurgical Sectioning

CSX¹ generously volunteered to make available several lengths of rail that were amongst those planned for replacement. Engineers from Loram and Rohmann, who used the RSCM and Draisine respectively, measured crack depths on rail at thirty different locations, and marked out thirty one-foot sections of rail for removal (see section B.1 for details). These were eventually removed by CSX and stored in Evansville, Tennessee. Of those samples, twenty were then shipped to the NRC facilities in Ottawa, where eight samples² were subjected to sectioning and

¹ Through Bill Bell, Manager of Contract Services

² NRC analyzed samples 2, 4, 6, 7, 12, 14, 16, 18. MRX analyzed samples 1, 30 and 33.

physical measurement of crack depths. That work is detailed in Appendix B. An example is given in Figure 1. Rail samples were cut by water jetting³ to provide a face of sufficiently good surface finish, which enabled dry dye penetrant enhancement for highlighting cracks and depth measurement. Liquid particle enhancement was also performed on some samples and was found to provide a clearer picture of the cracks.

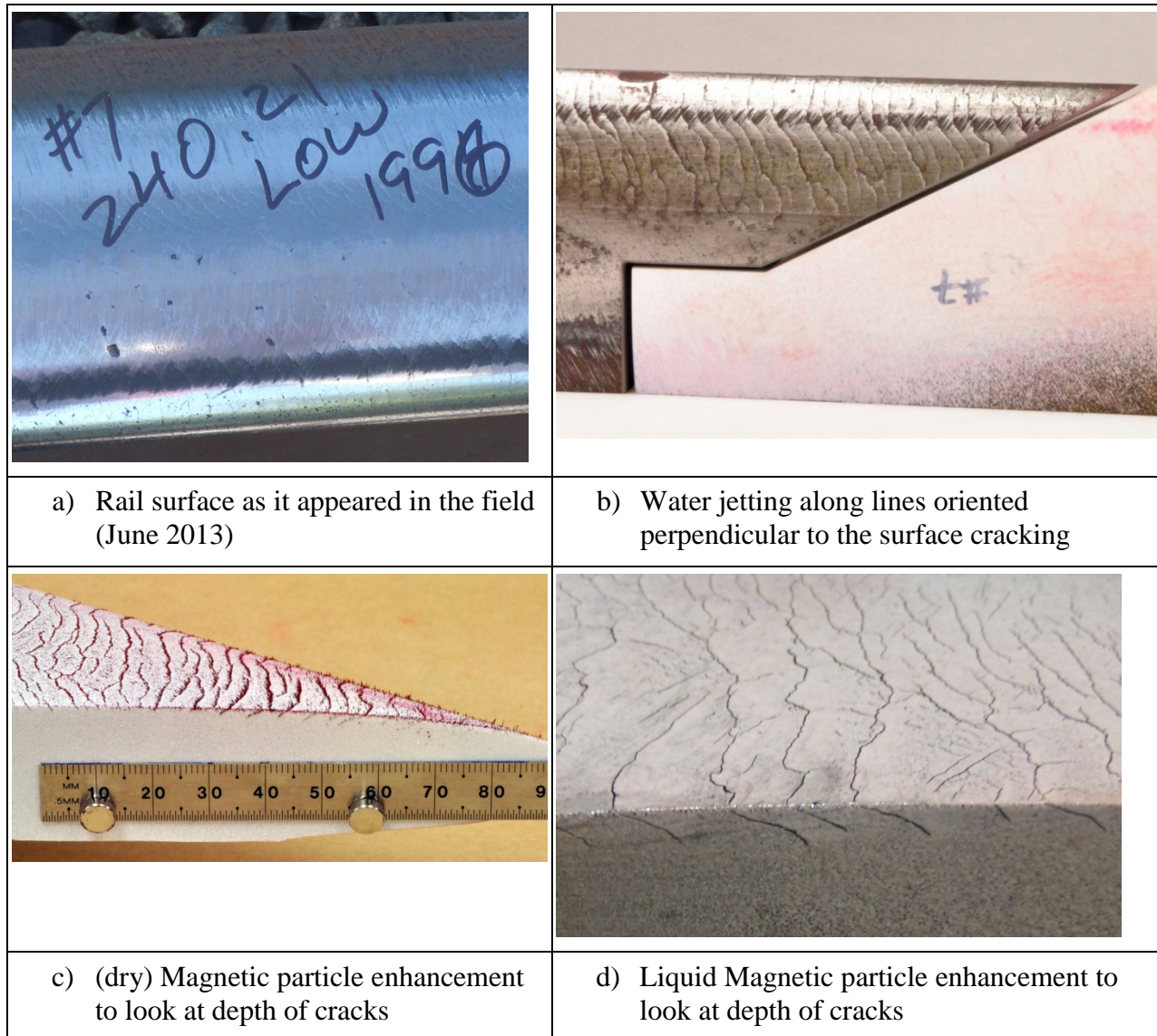


Figure 1: The process followed for determining the depth of the surface cracks.

An early comparison of the field-measured crack depths with the water jetting slices proved discouraging. Since the water jetting only captured a couple of the longer cracks in most cases, a second method was employed. Following the process used by MRX, NRC progressively milled away the crown of the rail in 0.4mm increments, with photographs of the magnetic particle

³ A very first sample was cut with wire EDM but the melting process involved “healed” the cracks on the cut face so that they could not be measured.

enhanced cracks being collected at each height. Samples 7 and 14 were processed in this way with a total of thirteen and fourteen milling cycles being conducted, respectively. Subsequent processing of the images in a 3-D Computer Aided Design (CAD) package enabled the envelope of the deepest cracks to be evaluated. For sample 7, water jetting had given a crack depth of 2.0 mm (see Figure 1) while the milling method resulted in a depth of 2.1 mm. A third effort involved additional water jetting sections along the length of samples 6, 12, 16 and 18. Additional depth measurements were taken and gave greater confidence in the sectioning results. Upon completion of its first set of sectioning work, NRC shipped the remaining whole rail samples to the University of Alberta in Edmonton for further study. Three samples (numbers 1, 30, 33) were shipped directly from Evansville to the MRX facility in Australia for their further study. Those three samples were milled by MRX and the resulting measurements included with the NRC samples in Table 1 and Figure 3.

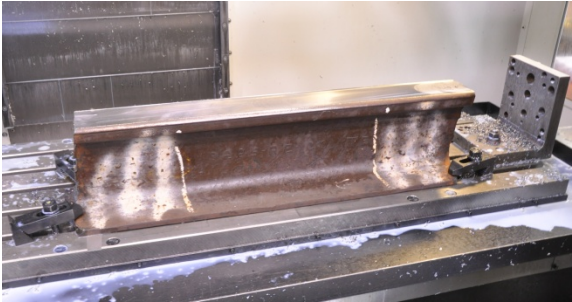
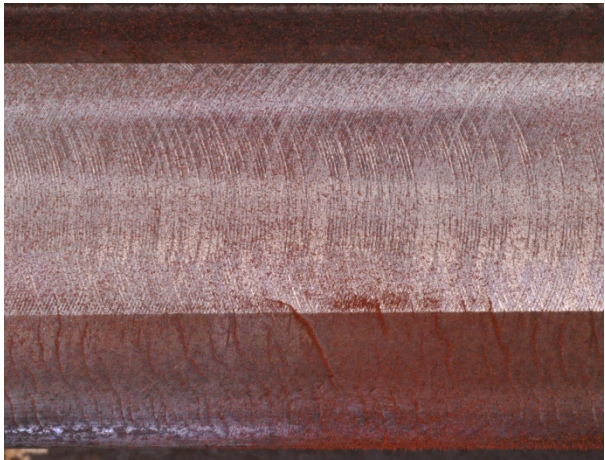
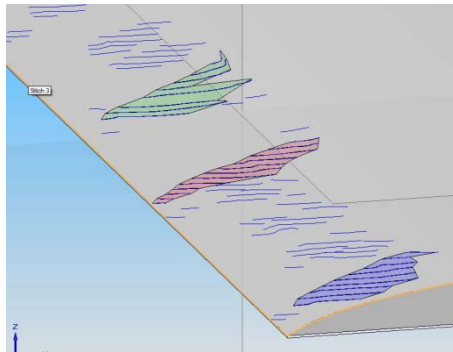
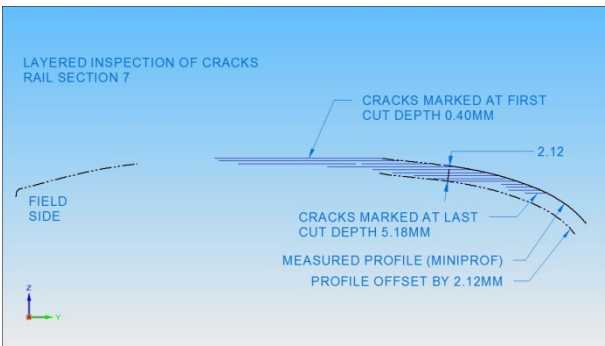
	
<p>a) Setting up on the milling machine to remove a skim of metal from the top of the rail</p>	<p>b) Magnetic particle enhanced photographs of the exposed surface</p>
	
<p>c) Importing images into Solid Edge and tracing cracks</p>	<p>d) The outer envelope of the cracks is believed to represent the greatest depth of cracking along the length examined</p>

Figure 2: The process to mill and chase cracks through the rail head.

The validation results were then summarized (Table 1) and provided to Loram, MRX and Rohmann. It should be noted that the maximum depth measureable by the RSCM is 7 mm, while the Draisine is limited to 5 mm. The two units showed general agreement except for samples 2 and 4. That discrepancy was dismissed as likely resulting from the measurements being recorded at different sites. Unfortunately, none of the measurements correlated well with the sectioning outputs. For Samples 7 and 14 that were milled, the sectioning values of 2-3 mm should be quite reliable but both units measured very deep cracks of 5 mm or greater. Samples 16 and 18 were an exception in that the RSCM predictions were “reasonably close” to the sectioned values determined for these older rail steels. This raised the possibility that the RSCM is affected by rail metallurgy, even though previous experience had suggested that it wasn’t.

Table 1: Summary of results for RSCM and Draisine measurements vs measured cracks depth through rail sectioning and milling

#	Rail Manufacturer	Rail Weight	Rail Year	Rail Notes	Location	Degree of Curve	Rail Side	RSCM (mm)	Draisine (mm)	Meas.	Method
1	Beth Steelton	136	1997		220.45	2°0'	Low	4.5	4.1	2.02	milling
2	Nippon		1996	VT	224.45	4°0'	Low	0.1	2.2	1.2	water jet
4	Nippon		1996	VT	224.45	4°0'	Low	0.1	5	1.1	water jet
6	Beth Steelton	136-10	1994	CC	226.68	2°0'	High	4.3	3.5	2.3	water jet
7	Beth Steelton	136-10	1996	CC	240.21	3°0'	Low	6.3	5	2.12	milled
12	Tennessee	132	1975	CC	247.79	0°0'	Right	6.9	5	3	water jet
14	Tennessee	132	1975	CC	259.05	0°0'	Left	4.8	5	2.87	milled
16	Tennessee	132	1957	C rail	259.05	0°45'	Low	2.1	no meas.	1.65	water jet
18	Tennessee	132	1967	D rail	259.05	0°45'	High	1.3	no meas.	1.2	water jet
30	Tennessee	132	1960	CC	266.92	2°0'	Low	7	5	3.31	milling
33	Tennessee	132	1960	CC	265.59	1°15'	Low	1.6	no meas.	1.83	milling

Since MRX completed its work in Australia with the three North American samples (1, 30 and 33) it continues to examine samples from around the world to understand the differences.

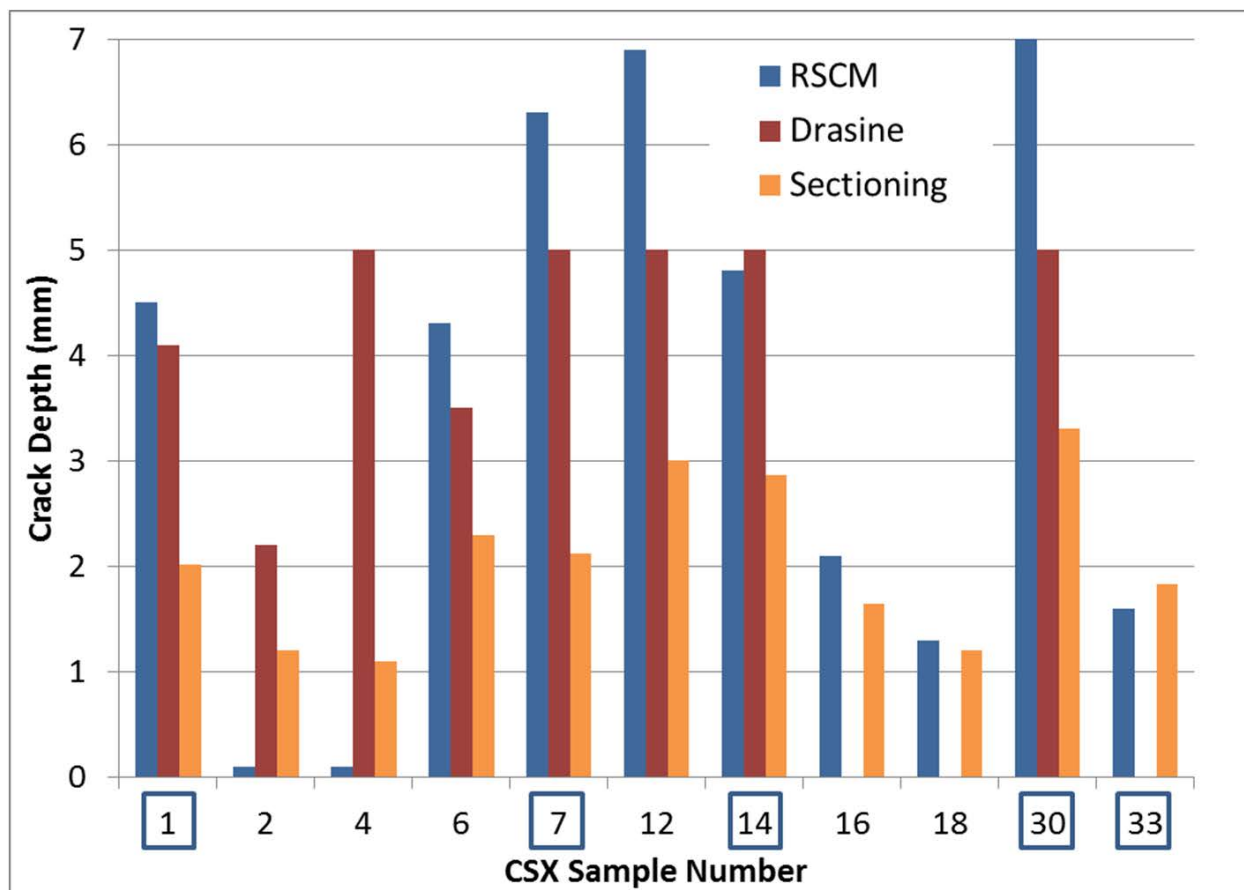


Figure 3: Comparison of crack depth measurements obtained with the MRX and Rohmann systems with those obtained through destructive sectioning and milling. The milled samples (which should be the most reliable) are highlighted with the blue box.

Besides the possibility of measurement faults, there are two theories for the poor correlation:

1. The sectioning process failed to capture the true depth of the deepest crack. There is merit to this theory since the sectioning approach looks at only a small sample of the cracks available in the short piece of rail. Furthermore it is unlikely that the fullest length of any crack will be seen by the sectioning since it likely has its longest projection along a plane that is different than the one it is being viewed along. For this reason, the sectioning results can always be expected to under-estimate the true depth.
2. The measurements and rail sections are simply from different locations due to errors in record keeping.

With respect to the second cause, it was decided that a repeat set of measurements and sectioning work was needed, and that better book-keeping would be employed.

3.2 Pre and Post-Grinding Measurements on CSX

Loram with CSX arranged for the project team to be on track near Ashland Kentucky as the rail grinder passed through that area. The grinding plan was reviewed and track locations where

multi-pass grinding was planned were identified. When multi-pass grinding was used, typically three grinding passes removed roughly 0.5 mm from the rail crown, but in one case 6 grinding passes were made and nearly 1.5 mm of metal was removed from the crown.

Each site was marked at 6-8 points between two welds, each having a weld in the middle as well. They were marked out using a 25 m tape measure at distances corresponding to unit metres. These are summarized in Table 2.

Table 2: Seven curves were measured on the CSX railroad before and after rail grinding.

MP	Curvature	Metallurgy		# of passes		# of sites
		High	Low	High	Low	
CA 553.54	0.5-1.0°	122 CB Krupp 1980		3	2	6
CA 551.65	1°	122 Klockner 1980		6		8
CMG 4.37	5°		136-10 Beth 1998		3	5
CMG 8.0	4°		141 VT ISG 2005		3	4
CMG 11.0	4°25'	136 RE VT Mittal 2011	136-10 Beth 1998		3	4
CMG 12.33	6°35'		136-Beth 1998		3	4
CMG 33.5	8°25'	141 VT ISG 2004	141 Beth 2001	3	3	4

Photographs and profiles were collected at each of the 4-8 measuring points on each rail. The extent of the curve, including those sites, was measured by both the Draisine and RSCM instruments. The one exception was CMG 4.37 where post-grind crack depths were only collected by the MRX-RSCM unit.

The metal removed during grinding was calculated as the difference between the pre- and post-grind MiniProf rail profile measurements. The depth of metal removal from grinding was found by using plots provided by Loram (see Figure 4) showing the transverse rail profiles before and after grinding. The plots also provide the depth of metal removal over the whole grinding surface. This information was converted into three values of metal removal depth that are function of the area on the rail: gauge, field and ball (or crown). These values were obtained using the following rules:

- The gauge region is measured from the gauge (right) edge of the profile up to 20 mm towards the crown of the rail (green area in Figure 4). The largest value in that zone is taken as the gauge metal removal depth.
- The field region extends from the field (left) edge of the profile up to 20 mm towards the crown of the rail (red area in Figure 4). The largest value in that zone is taken as the field metal removal depth.
- The ball region is taken as the area between the gauge and field zones and corresponds to the non-colored area in Figure 4. Contrary to the gauge and field areas, the metal removal depth is equal to the lowest depth attained by the grinder. Taking the lowest depth is more relevant when studying the impact of grinding on crack depth in this area.

- Any spikes that appeared to be caused by surface contamination were ignored.

The results are summarized in Table 3.

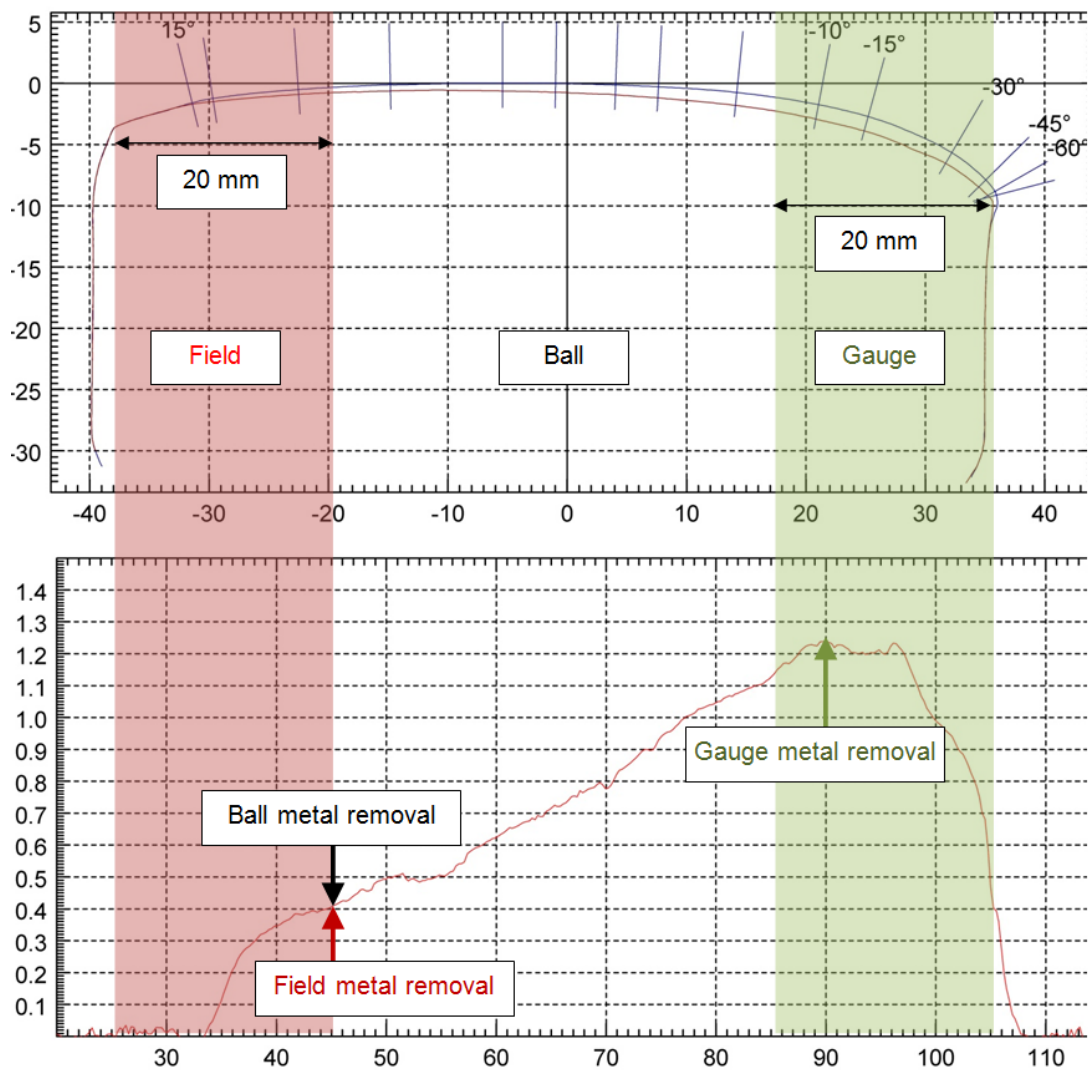


Figure 4: Method for evaluating the depth of metal removed at each test site⁴. This is a low/inside rail example.

⁴ This figure was developed by Stephanie Klecha of MRX.

Table 3: Depth of metal removed by rail grinding.

MP	Passes	Depth [mm]					
		High			Low		
		gauge	ball	field	gauge	ball	field
CA 553.54	3H / 2L	0.58	0.16	0.96	0.70	0.32	0.38
CA 551.65	6H	1.43	1.13	1.13			
CMG 4.37	3L				0.63	0.38	0.75
CMG 8.0	3L				1.23	0.55	0.55
CMG 11.0	1H / 3L	0.26	0.16	0.01	0.92	0.42	0.71
CMG 12.33	3L				0.74	0.47	0.68
CMG 33.5	3H, 3L	0.96	0.36	0.69	1.14	0.04	1.30

Rohmann and MRX each processed their pre and post-grind crack measurements and determined statistically the “delta” in the measured crack depth. An RSCM example is shown in Figure 5. With its 19 sensors, the RSCM unit measures across the rail head. The Draisine meanwhile has four probes that, while moveable, typically are placed near the gauge corner (see Figure 6). The Draisine crack depth measurements were reported for the gauge corner only of both the high and low rails.

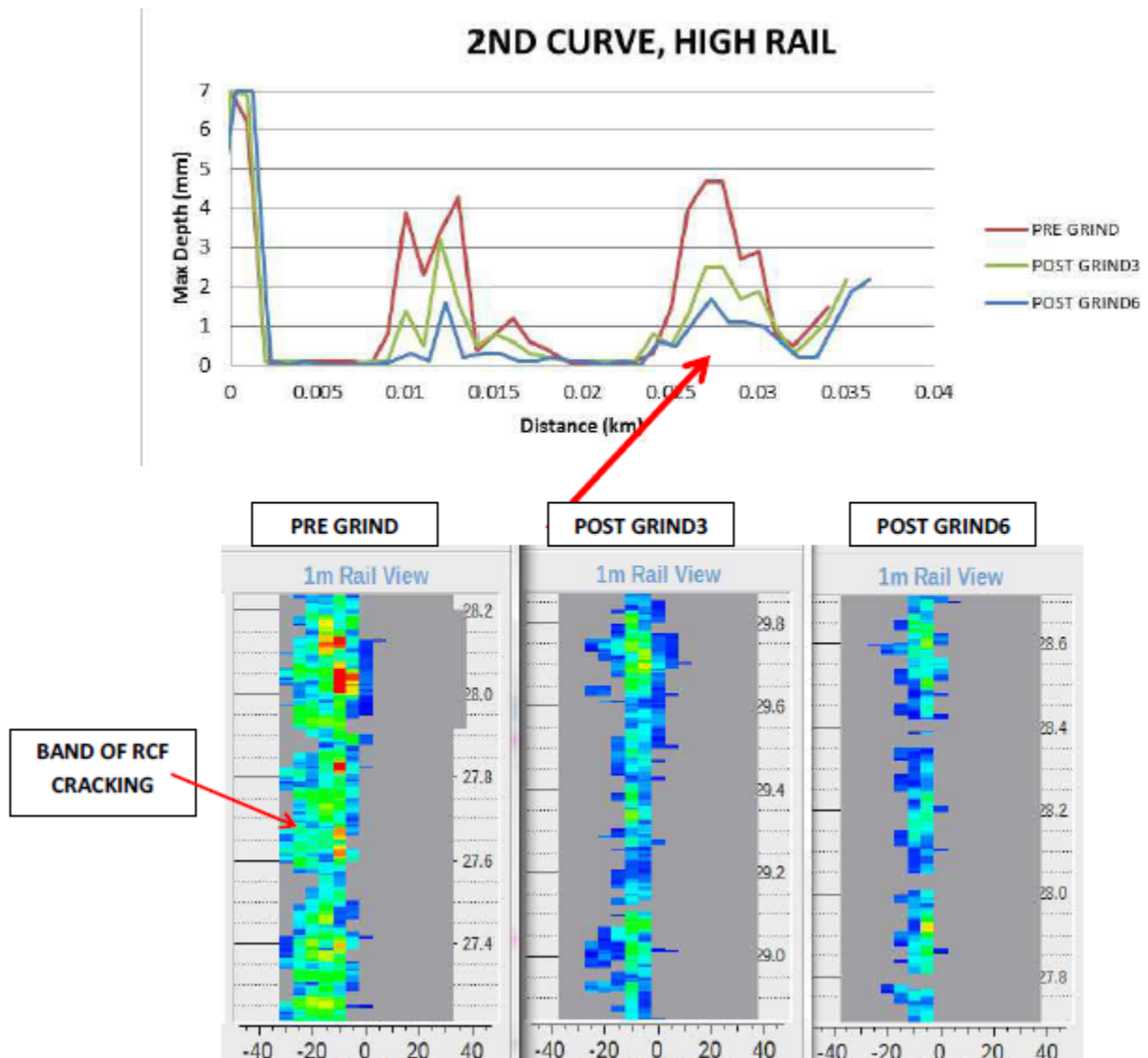


Figure 5: Example of RSCM data showing crack depth measurements.

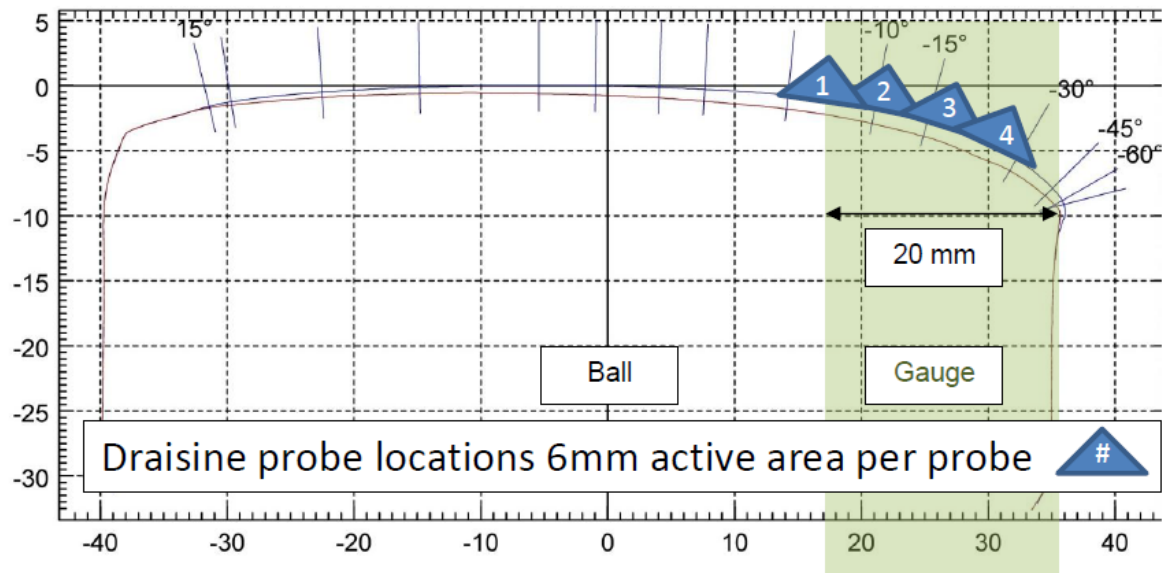
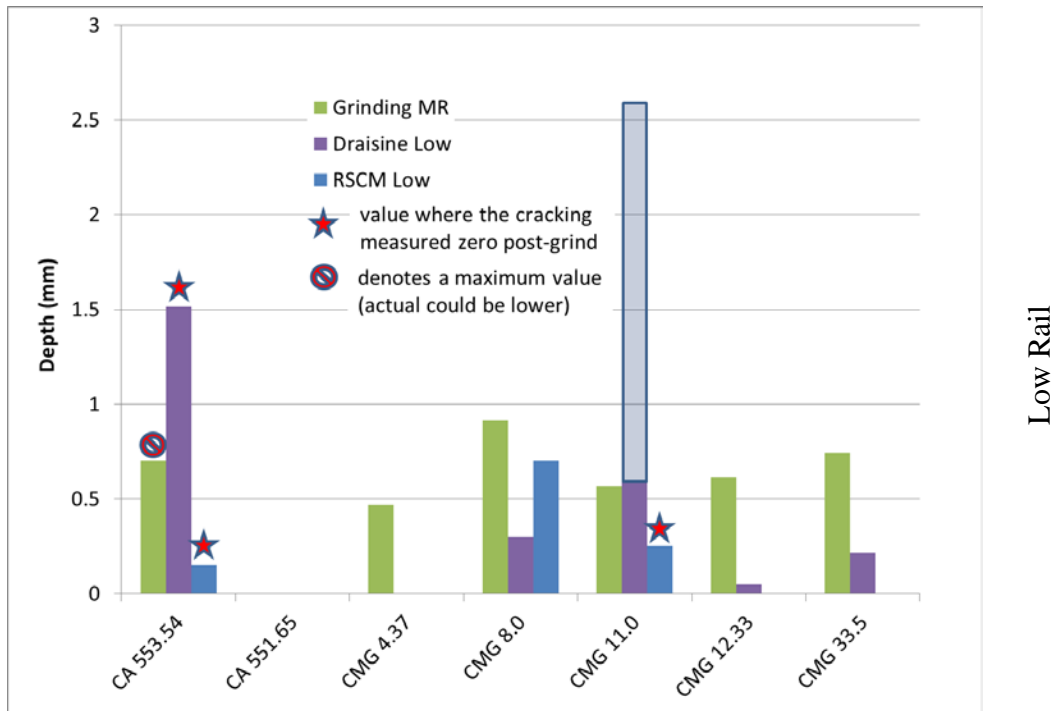


Figure 6: Although the 4 probes on Rohmann's Draisine can be repositioned, they are commonly left at a gauge corner position, even on low rail measurements⁵.



⁵ Figure courtesy of Eric Eberius of Rohmann.

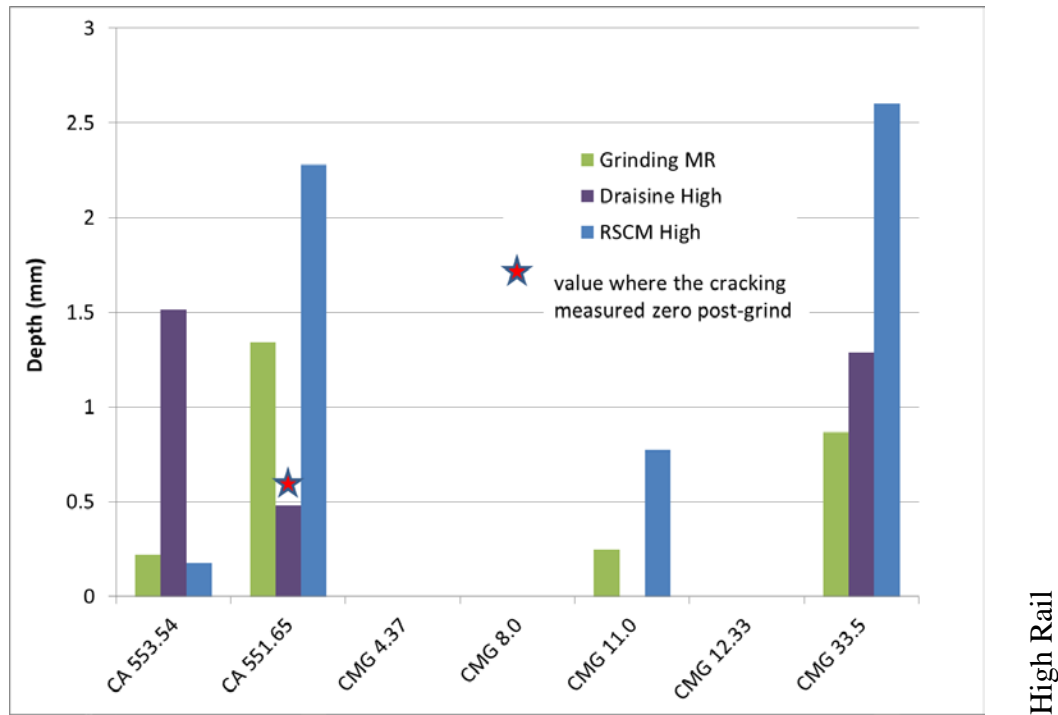


Figure 7: Results of CSX rail grinding tests – metal removed by grinding is compared with the measured shortening of the cracks. The asterisk denotes cases where the final crack depth was zero.

3.3 NS Hardy Curve Samples

After completing the CSX work, the team moved to Roanoke, Virginia to inspect and measure the 5.7° Hardy curve on the Norfolk Southern Railroad (Figure 8). This is an NS test site where the November 2013 grinding cycle had been deliberately skipped on the low rail to cause longer/deeper cracks to develop and to provide a greater range of conditions for the measuring systems. It is estimated that 35 million gross tons (MGT) had passed since the previous grinding cycle. The low rail was removed from service two weeks after the measurement program and a total of eight samples collected from the rail for further examination. Three of them were sectioned or milled for this study.

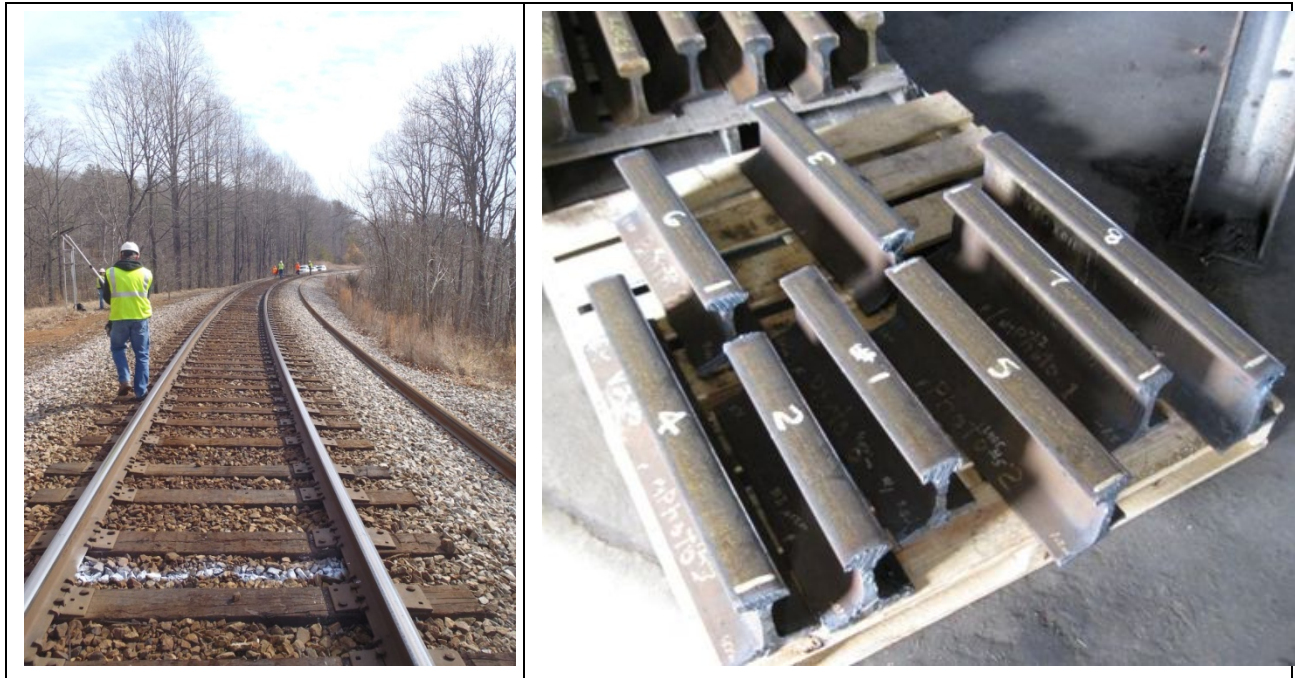


Figure 8: The Hardy curve on the Norfolk Southern Railways is 5.7°. The low rail was last ground June 2013 and the high rail on November 2013. The low rail was removed from service two weeks later and eight samples removed.

The condition of the rail varied significantly throughout the curve with short sections exhibiting only minor RCF and others showing heavy RCF and pitting. This is illustrated by the RSCM scan of Figure 10 which finds cracks varying from 0 to more than 7 mm deep.

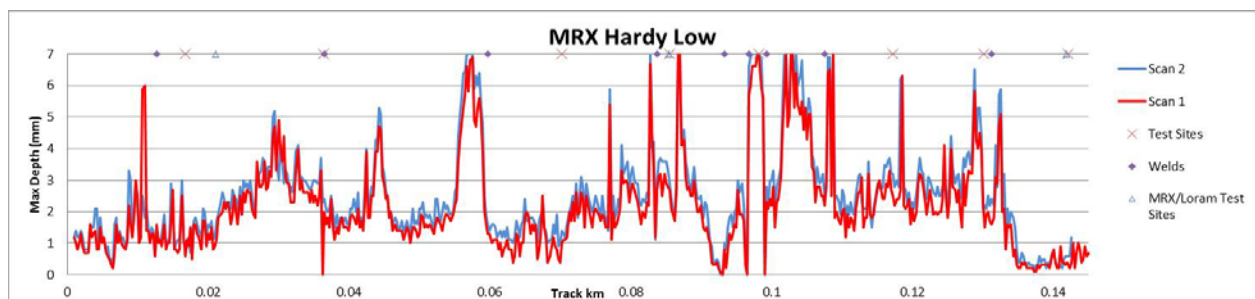


Figure 9: Two scans of the RSCM unit over the Hardy curve, with test site locations marked.

NS Laboratories analyzed three of the rail samples. Examples of the metallurgical sections and crack measurements are shown in Figure 11.

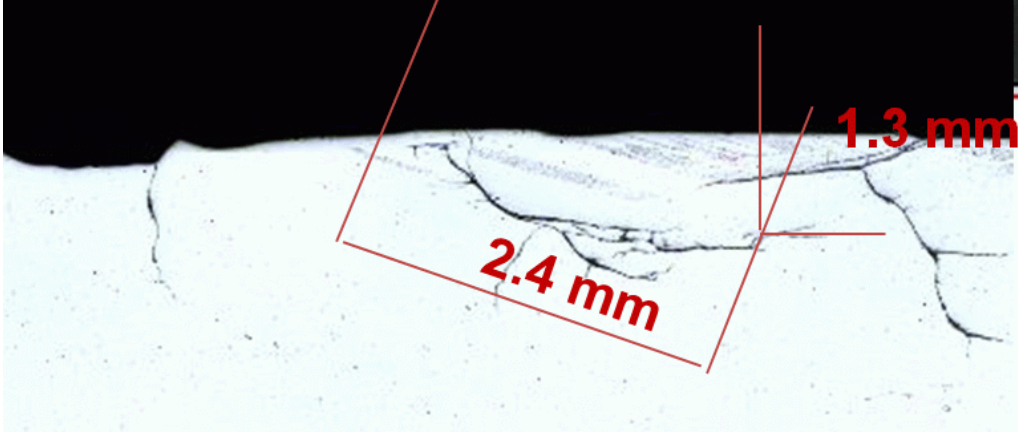
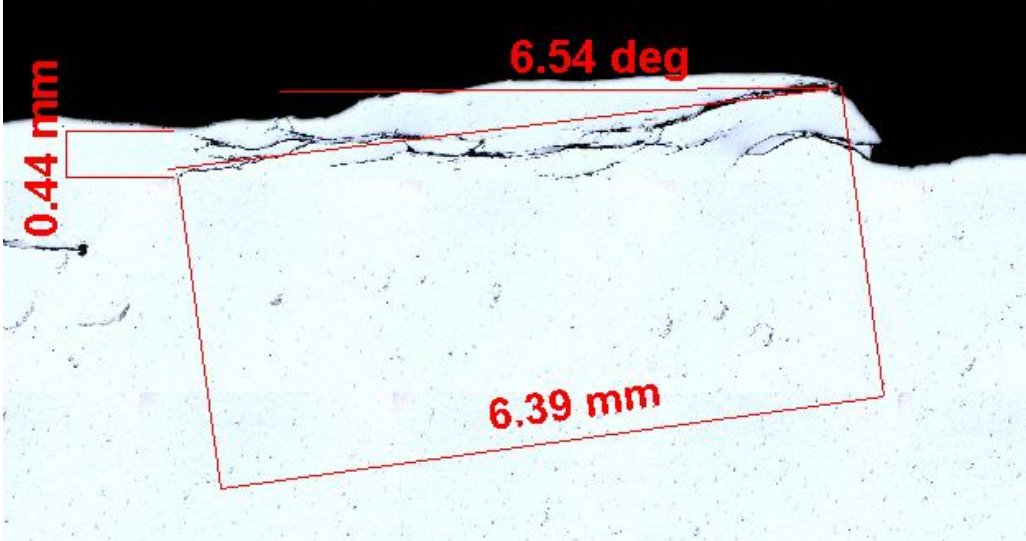
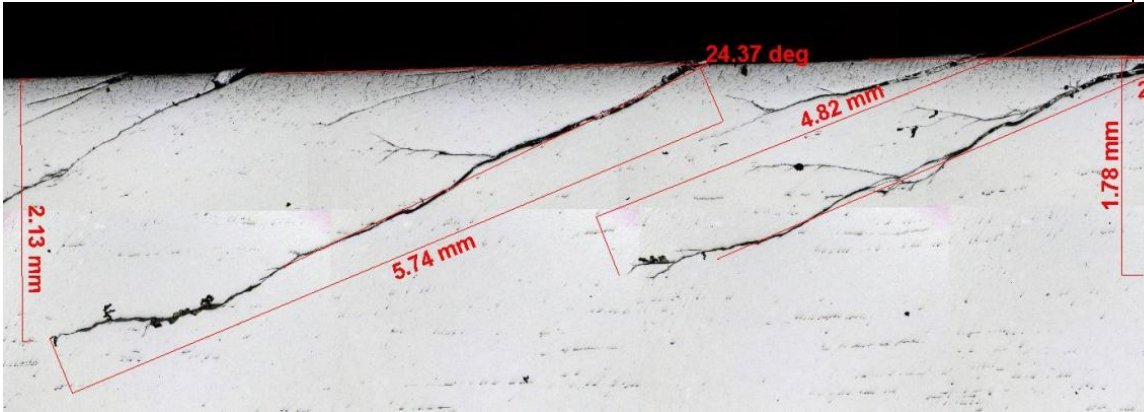
	<p>Sample 4 (cross section)</p>
	<p>Sample 5 (cross section) (Milling showed a depth of 2.3mm)</p>
	<p>Sample 6 (longitudinal)</p>

Figure 10: Sectioning of three rail samples and crack measurement were undertaken by NS Labs.

Sample 5 was also subject to milling (see section B.3.2). Analysis of the NS photographs shows that the “true crack depth” is about 2.3 mm, compared with the value of about 0.5mm given by the selected cross section (shown in Figure 10).

A comparison of the measurements from Draisine, MRX-RSCM and NS is in Figure 11. The Draisine and RSCM measurements showed general agreement with each other, but they over-predict the NS depth measurements by 50-100%.

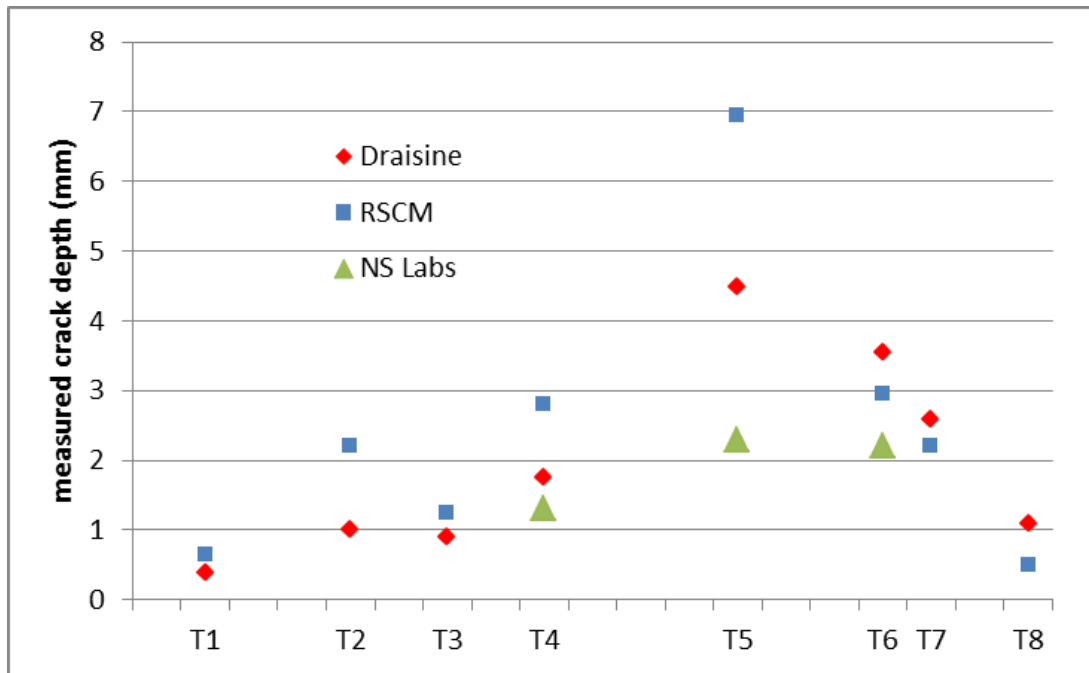


Figure 11: Summary of results for measurement versus machining of rail samples on NS Hardy curve.

The results of this work were presented by NS in May 2014 [4]. It was suggested that the Draisine can measure the crack length properly but since depth is predicted by assuming a propagation angle, significant errors in depth can arise if the propagation angle varies significantly from the assumed value. In several of the samples, the propagation angle was found to be lower than the assumed value of 27 degrees, which contributed to the over-predictions.

3.4 BNSF Staples Subdivision – measurements versus milling

BNSF Railway (BNSF) had volunteered early in the program to provide rail samples for measurement and analysis. This offer was accepted in the fall of 2014. In late November, NRC and BNSF inspected rail scheduled for replacement on the BNSF Staples Subdivision. Several rail samples were identified and marked out for extraction and subsequent shipping to Loram’s technical center in Hamel Minnesota. Each sample was between 18 and 30 inches in length. A range of RCF severities were represented by the samples. Both high and low rails were collected, along with some tangent rails near crossings. The rail surfaces were protected and so at the time measurements were undertaken, the running surfaces had not rusted.

These rail samples were set end to end in two strings, with the gauge side set to the outside. Rails were shimmed as necessary to provide a satisfactorily smooth running surface. A schematic

of the setup, with some details for each sample, is shown in Figure 12. Additional details for the samples is available in Appendix B.4

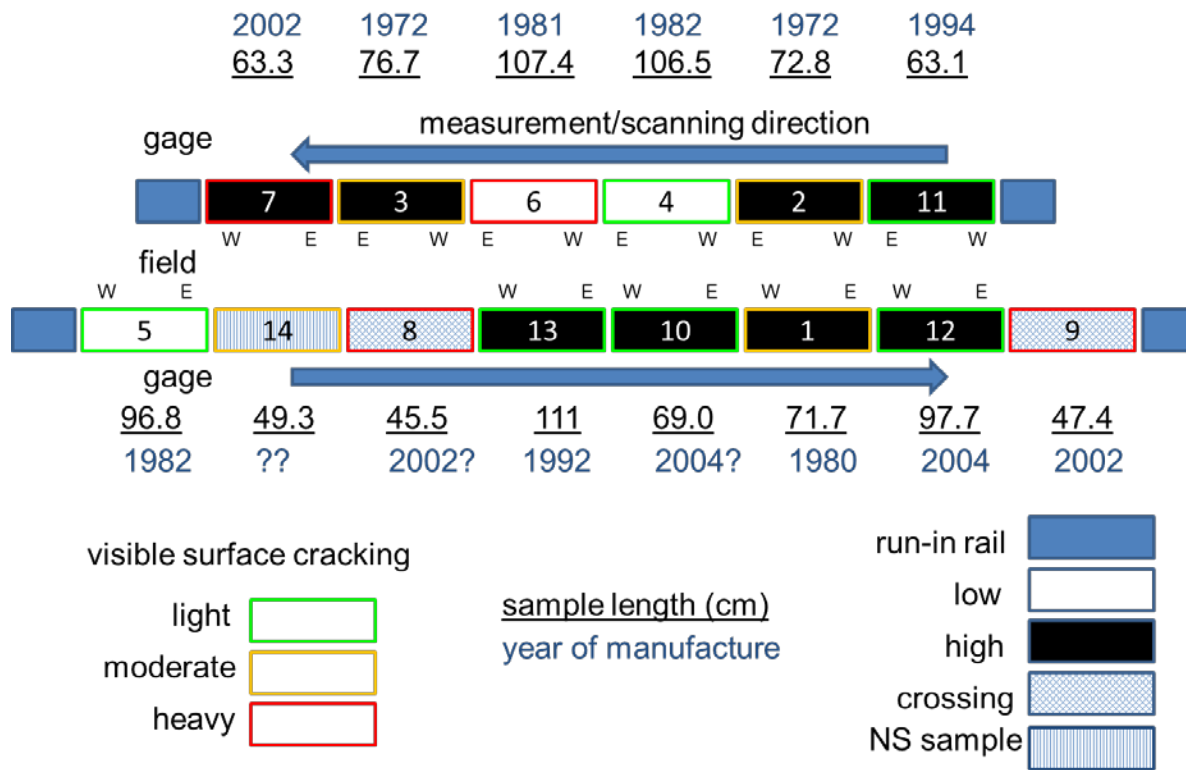


Figure 12: Layout of BNSF Staples samples for measurement with the walking sticks.

On February 2nd, 2015 representatives from MRX, Sperry, BNSF, CSX, CN, FRA, NRC and Loram gathered in Hamel to witness the Rohmann and Sperry measurements. Rohmann had unfortunately been delayed by bad weather, but was able to later collect measurements on February 19th. Upon completion of those measurements, the running surfaces were protected with grease and the rails bundled on a pallet. These were then shipped to the University of Alberta where rail milling was undertaken. Details of that process are given in Appendix B.4

A summary of the results is shown graphically in Figure 13. Based on the previous experience, Rohmann suspects that considerable uncertainty exists around the true crack propagation angle and so has started to report instead on crack depth. For the purpose of this effort, values were provided for crack propagation angles of 15, 25 and 35 degrees. These are all shown in Figure 14 as indicated by the legend on the left side of that figure. All systems reported heavy cracking on samples 8 and 16, but remain inconsistent for light and moderate cracking. In contrast with previous efforts (e.g. Figure 7 and Figure 11) where the Rohmann and MRX tended to over-predict crack depth, for samples 3, 4 and 6 the estimates were generally low.

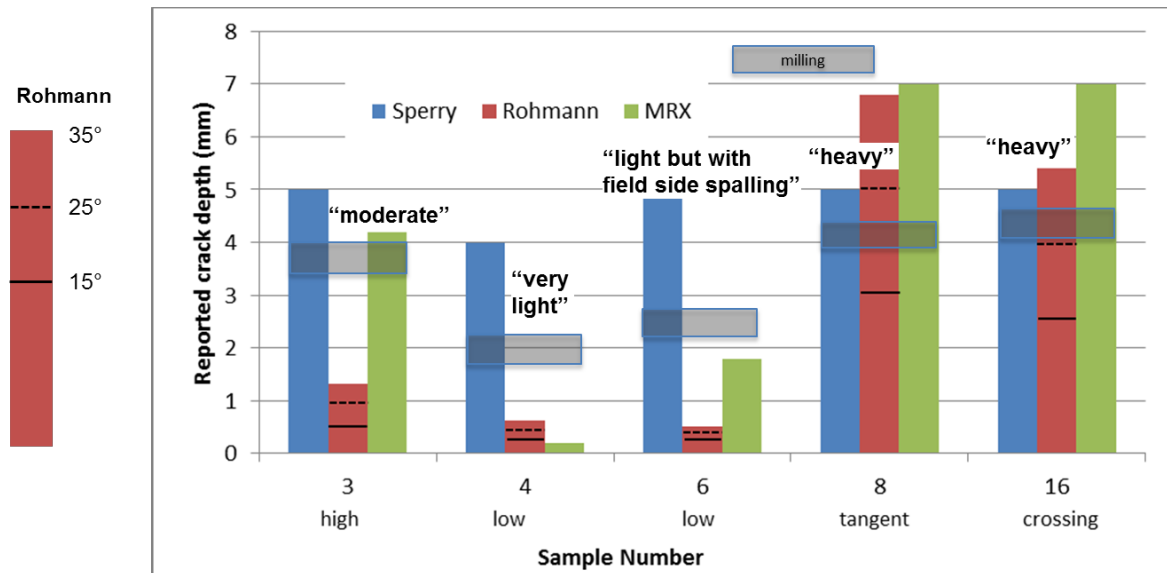


Figure 13: Comparison of electromagnetic measurements with milling results.

3.5 A Transit Example

During a recent NRC project in Asia, the Draisine unit was used to inspect rail prior to grinding. At one test location the Draisine reported 2 mm deep cracks prior to grinding. After grinding the reported depth was 0.25mm, suggesting that 1.75mm of metal had been ground from the gauge corner. Analysis of the rail profiles found that a maximum of 0.88 mm of metal had been ground from the gauge corner, roughly half the eddy current measured value.

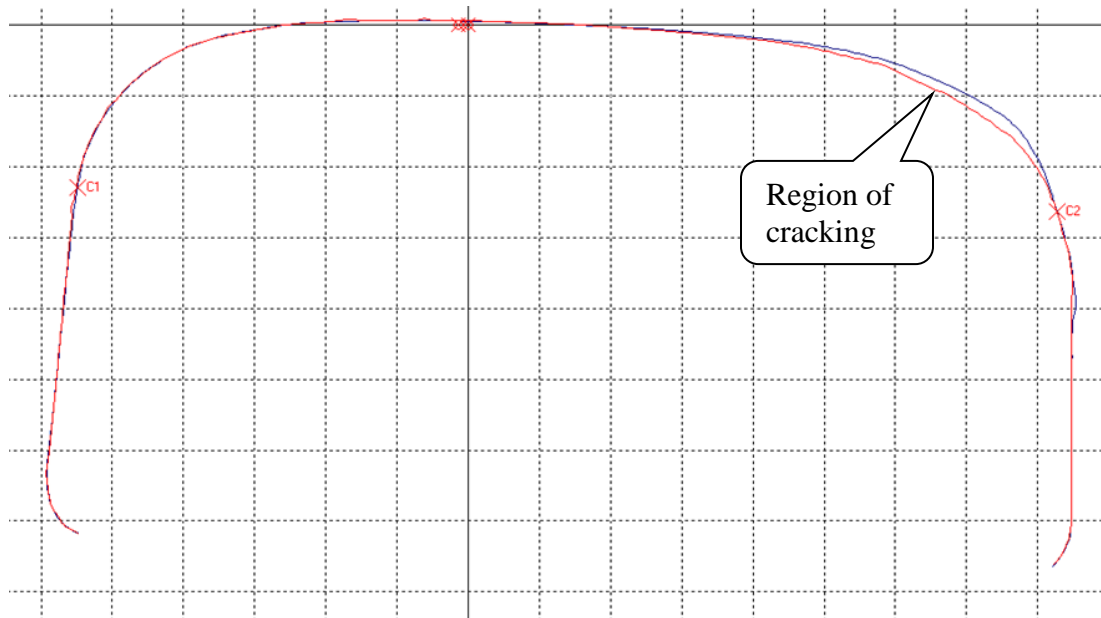


Figure 14: Difference between the pre- and post-grind rail profiles shows that 0.88 mm of metal was removed from the gauge corner.

4. Conclusions

A) Several different approaches were undertaken to compare the “real” depth of surface cracking with measurements of crack depth. These are summarized below:

Method	Description	Results
CSX – rail samples	Machine measurement of crack depth prior to rail removal at marked locations. Compared with values obtained through metallurgical sectioning.	Figure 3: RSCM and Draisine return similar values for heavy cracking, but these values are often double the value obtained from milling or sectioning. RSCM shows good agreement with “old” 1960’s steels (samples 16,18 and 33).
CSX – Rail grinding tests	Pre- and post-grind measurements of change in crack depth, which were compared with amount of metal removed.	Figure 8: The results were inconsistent and the correlation poor for both devices.
Norfolk Southern 5.7° Hardy curve	Repeat measurements at eight locations through the curve.	Figure 12: Draisine and RSCM in general agreement with each other, but over-predict depth by 50-100%.
BNSF rail samples	Machine measurement of crack depth in laboratory setting. Compared against values obtained through milling of the rails.	Figure 14: All systems correctly identified deep cracking (>4mm) but were inconsistent with moderate and light cracking.
Asian Transit System	One location before and after grinding.	Section 3.5: Draisine prediction of crack depth reduction was twice the actual metal removed.

B) In general the correlation between machine predictions of crack depth and other measures to know the “real” crack depth have been poor. Possible explanations include technical limitations of the instrumentation as well as difficulties in determining a “true” measure of the crack depth.

Technical Limitations

- In a field setting it is difficult for the eddy current systems to get a good calibration. Ideally there would be available a clean length of rail on hand with the same manufacture

and hardness as the tested rails on which to perform the calibration. Calibrating on damaged rail to measured damaged rails is a poor alternative but is unfortunately most common.

- Eddy-current-systems measure crack length, but for customer purposes report crack depth. One of the investigations suggests that the eddy current measurement of crack length might be quite reliable, with errors arising when that length is transformed into a depth based on an assumed propagation angle. In the chiefly European systems on which the eddy current units were originally developed, there was some regularity to the cracking and crack angle to the surface that does not appear to apply to North American freight systems.
- All the electromagnetic systems are poor in sizing cracks that have a strong longitudinal component. Only when those cracks are severe enough to have initiated shelling - such that there is some component perpendicular to the measuring direction – will it be measureable.
- The effect of multiple cracks, crack angle and crack shape (e.g. long and narrow versus wide and shallow penny cracks) on eddy current crack measurement is not well understood and may be affecting the reliability of measurements.

Determining the True Crack Depth

- Whereas the walking sticks generally report the deepest crack every meter, many of the metallurgical samples were less than a meter in length. It is very possible that the metallurgical approaches failed to find the deepest crack that was reported by the RSCM and Draisine in the first three studies. Also, as the NS milling example of Section B.3.2 shows, the results from a cross section can be very different from the milling values (0.5mm versus 2.3mm for milling in this case), with the latter believed to be more accurate. The last milling work, undertaken on the BNSF samples, should however be very credible since the samples were of sufficient length and the milling work quite detailed.
- C) Although the electromagnetic systems are working well in Europe to quantify crack depth, reliable measurements of surface crack depth and growth rate on in-service “North American” rails are not yet available. The chief reasons are:
- An inconsistent crack propagation angle, with values varying from nearly 90 degrees to the surface on some low rail cracking to very low angles (e.g. 6.5 degrees). This is problematic for the eddy current systems, though it has no known influence in the magnetic flux systems.
 - All of the systems were originally developed with a focus on gauge-corner cracking - chiefly of high rails – that is prevalent in European and Asian systems. Low rail cracking is a significant concern in North American freight operations. The field side location of much low rail cracking demands that sensors be present at that position across the rail. Measuring these strongly longitudinal cracks will require further advances by all the vendors of electromagnetic systems.

- Differences in rail metallurgy are likely to have some influence, since higher hardness and hyper-eutectoid rails may influence readings compared to the softer eutectoid steels analyzed during the bulk of the development efforts.
- D) The original impetus for this work was to identify and validate a crack measuring system that could support the development of an “Atlas of Rail Surface Fatigue”. The atlas intended to correlate visible surface damage with measured depth of damage over a very broad range of samples, and thereby enable credible, data-based classifications of light, moderate, heavy and severe cracking. Any information on crack initiation and growth rates was further to be leveraged by an ICRI (International Collaborative Research Initiative) project aimed at “Quantifying the Magic Wear Rate”. In the absence of measurement accuracy, these two efforts become much more difficult to achieve.
- E) While accuracy in measuring absolute crack length was not demonstrated in this project, the measurement systems did all record stronger signals at greater levels of surface damage, and so the trends are credible: over time and traffic damage to the rail is seen to increase (see for example Figure 15) while with grinding the damage levels decreased. So there is currently application for their use as a maintenance prioritization tool and for trending damage over time.

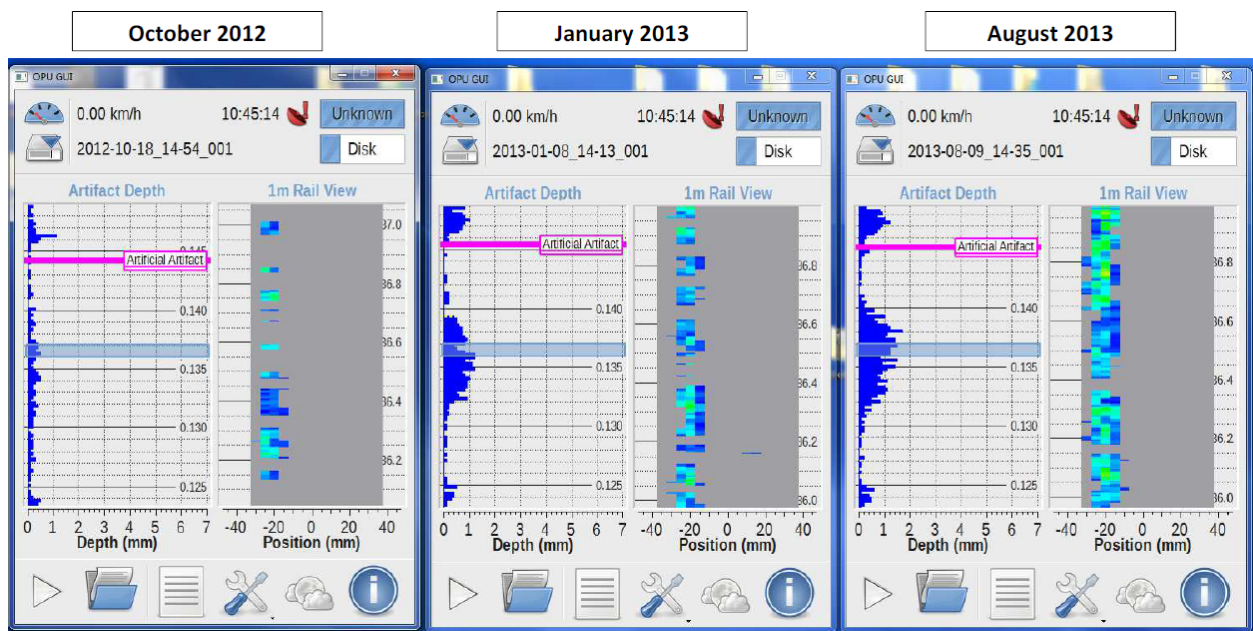


Figure 15: The progression of damage as measured with the MRX RSCM. The depth and extent of cracking is seen clearly to grow with time.

- F) The collaborative team that enabled this project included 3 railroads (CSX, NS, BNSF) and 4 suppliers (Loram, MRX, Rohmann, Sperry). All participants recognize the opportunity and promise provided by crack measurement tools and all appear willing to engage in additional work.
- G) Further development of electromagnetic tools for measuring surface cracking in North American freight rail steels is required. Some possible topics are proposed:

- Given the wide variation in damage morphology on North American freight railroads, there remains a need to continue broad surveys and milling of rail samples, especially low rail samples, to support the theoretical and practical studies aimed at continuously improving the accuracy of the measurement systems. These may eventually enable solid assessments of absolute damage depth such as are common now in Europe and Asia.
- Field studies are required to improve understanding of the limitations and applications of the various walking stick and hy-rail based systems for managing rail surface fatigue. For examples:
 - Applications of the trending capabilities to understanding the effectiveness of rail grinding, friction management and rail replacement.
 - Correlations between measured surface damage and broken rails.
 - Understanding the difference in growth rates of ground (but not removed) cracks and those that have been freshly initiated.
- Ongoing review of fundamental studies that are considering different propagation angles, crack shapes, and systems of overlapping cracks.

5. Acknowledgements

Bill Bell (CSX) – for sponsoring the various field work activities and accompanying the team over several days of measurements.

Eric Eberius (Rohmann) – for supplying the Rohmann Draisine and participating in the measurement program, analyzing data and reviewing project outcomes.

Bob Harris (LORAM) – for supplying the MRX RSCM instrument, organizing all field work and coordinating with the LORAM rail grinders as required. Also for setting up and hosting measurement of the BNSF rail samples.

Babak Hassas Irani (University of Alberta) – for performing milling and photography of several BNSF rail samples.

Jay Holland (CSX) – for facilitating the storage and shipping of CSX rail samples to Canada.

Alok Jahagirdar and Alexandre Woelfle (NRC) – for helping to organize, manage and analyze the various data sets.

Brad Kerchof (Norfolk Southern Railroad) – for sponsoring track access and protection for a set of measurements on the NS and for undertaking metallurgical sectioning and analysis of the rail samples.

Stephanie Klecha (MRX) – for participating in the measurement program, analyzing data and reviewing project outcomes.

Dave Sheperd and Kristie Drawe (BNSF) - for supporting field inspection, removal and shipping of rail samples for subsequent measurement and analysis.

Ali Tajaddini and US FRA-DOT – for technical guidance and sponsoring the participation of the National Research Council, Canada in this work through grant #FR-RRD-0054-13-01-00.

6. References

1. E. Magel and K. Sawley, “Rail Surface Condition Alert – stage 1: Evaluation and calibration of surface crack measuring devices”, CSTT-RYV-CAT-090, November 2006
2. A. Dey, H. Hintze and J. Reinhardt, Operation of railway maintenance machines with integrated eddy current technique – an overview of new requirements in Germany, Proceedings, 11th European Conference on Non-Destructive Testing, Prague, Oct. 2014
3. E. Magel, “Rolling contact fatigue: a comprehensive review”, DOT/FRA/ORD-11/24, November 2011
4. Brad Kerchof, “Validating Rail Crack Measurement Devices on NS”, WRI conference, Henderson Nevada, May 7, 2014

Appendix A Details of the Surface Crack Measuring Systems

The family of electromagnetic based techniques includes:

- Eddy Current – electricity running through a coil generates magnetic fields in the adjacent conductive material that are disturbed by discontinuities.
- Magnetic flux leakage – the component is magnetized and the leakage of flux at discontinuities is detected with sensors near the surface.
- ACFM – a uniform electric current is induced into the component and the resulting magnetic fields are disturbed by surface breaking cracks that are detected by sensors above the surface.

Several commercially available walking stick systems exist (see Figure 17) that employ electromagnetic based techniques. They are battery powered for portability and are light weight, they are pushed manually by an operator, and they provide multiple probes to measure cracks across the rail head for single pass operation. A visual display provides direct reports, usually the length (or depth) of the largest defect over a metre (or yard) of rail length, and includes some count of the number of headchecks in that same metre. All are affected by welds and, therefore, can detect them. This can be considered fortuitous since it provides a good means for aligning repeat scans.

All units record data for later playback and include software for analysis. Although these systems can in principle detect subsurface cracks, they are optimized for surface breaking cracks.

Furthermore, all of the systems measure along the trajectory of the walking stick and do not see cracks that have a strong longitudinal orientation. A comparison of several of these systems is shown in Table 4.



Figure 16: The three electromagnetic based systems evaluated through this program.

Table 4: Comparison of features: MRX, Rohmann and Sperry walking stick devices

	Magnetic flux	Eddy current	Eddy current
	MRX - RSCM	EloRail WPG D340 Rohmann Drasine	Sperry Surface Crack Detection Walking Stick
URL	http://www.mrxtech.com.au/rail-inspection-monitoring/rail-surface-crack-measurement.html	http://www.rohman.com/uploadfiles/Draisine_10_GB.pdf	None yet.
Technology	Magnetic flux leakage	Eddy current	Eddy current
Measures	Crack depth, surface size and position on rail profile	Crack length. Calculates crack depth (surface to deepest vertical crack depth) based on assumed crack angle (25 degree normally, selectable from 2 – 90 degrees).	Crack depth into and crack length across the rail head surface
In dense cracks?	Returns deepest in specified section length, typically 1m	Maximum crack length per each 5mm of rail head is displayed	Maximum crack depth reported at configurable intervals along the rail. Intervals can be chosen from 10mm upwards
Range	Depth to 7 mm	Length to 12 mm (display limited) Depth to 5mm (display limited)	Length to 12mm. Depth to 5mm assuming a 25 degree crack angle. Expect better performance in future
# Probes across rail head	19	4 probes individually adjustable to a variety of positions on head (X2) and gauge corner (X2)	10
Probe Spot size	5mm pitch, covering full rail head width	6mm (24mm total coverage)	7mm spot size each, interlaced to give full head coverage
Weight	20kg (complete with battery)	39 lbs. / 17.6 kg (complete)	19.3kg
Affected by surface films?	No	No	No
Dependency on metallurgy	Negligible impact of metallurgy	Recalibration (<1 minute evolution) for some steel types during operation may be necessary if rail type changes significantly	Negligible variation in crack depth for different rail types.
Switch Measurement	Yes, but no manganese steel cast sections	Yes	Yes
Sensor to rail interface	Contactless, flat shoe with sensors. System measures rail profile and signals are adjusted for standoff	Ceramic shoe houses probes and shoe is spring loaded to maintain contact on rail head	Spring loaded sensors within a polyurethane tire which assists in keeping a constant liftoff
Allowable standoff from rail?	Standoff is maintained by the system wheels. System can see down to a maximum of 15mm profile drop	Probes to remain in contact with rail head at all times. Separation distance <2mm is critical	The weight of the stick keeps the required pressure of the probes on the wheel.
Operating speed	2-5 km/hr	0 to >Jogging speed	0 to 10 mph

Appendix B Validating Electromagnetic Surface Crack Measuring Systems

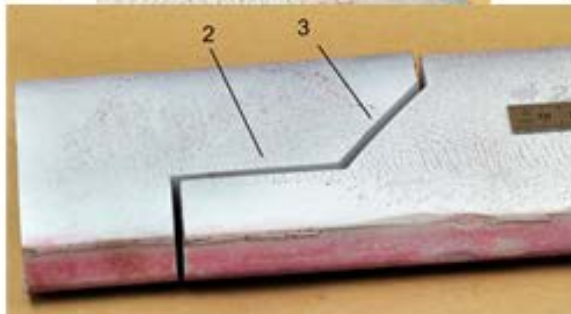
B.1 CSX rail samples from June 2013

Sample #	Rail Manufacturer	Rail Wgt	Rail Year	Rail Notes	Degree of Curve	Rail Side	Curve or Tangent Name	Latitude	Longitude (-)	Meters to Low MP Weld	Meters to High MP Weld	Meters from run start
1	Beth Steelton	136	1997		2°0'	Low	220.45	35.670400	81.980448	8.76	15.44	10.66
2	Nippon		1996	VT	4°0'	Low	224.45	35.623222	81.966600	2.87	20.93	75.87
3	Nippon		1996	VT	4°0'	Low	224.45	35.622942	81.966873	3.03	11.07	115.23
4	Nippon		1996	VT	4°0'	Low	224.45	35.622657	81.967085	1.37	None	151.07
5	Beth Steelton	136-10	1994	CC	2°0'	High	226.68	35.590560	81.975798	None	4.19	106.99
6	Beth Steelton	136-10	1994	CC	2°0'	High	226.68	35.590108	81.975955	23.47	0.63	55.23
7	Beth Steelton	136-10	1996	CC	3°0'	Low	240.21	35.425956	81.895475	None	12.13	141.73
8	Beth Steelton	136-10	1996	CC	3°0'	Low	240.21	35.425368	81.894927	19.69	4.21	62.11
9	Beth Steelton	136-10	1996	CC	2°0'	Low	238.3	35.448887	81.916685	4.30	19.50	35.10
10	Beth Steelton	136-10	1996	CC	2°0'	Low	238.3	35.448765	81.916617	17.86	5.94	48.66
11	Beth Steelton	136-10	1996	CC	2°0'	Low	238.3	35.448373	81.916360	19.05	4.85	97.55
12	Tennessee	132	1975	CC	0°0'	Right	T247.79	35.335377	81.841928	2.73	2.78	5.02
13	Tennessee	132	1975	CC	0°0'	Left	T247.79	35.334718	81.841947	5.45	6.35	75.15
14	Tennessee	132	1975	CC	0°0'	Left	T247.79	35.334602	81.841955	5.56	6.04	63.24
15	Tennessee	132	1975	CC	0°0'	Left	T247.79	35.334267	81.841972	7.55	3.95	26.35
16	Tennessee	132	1957	C rail	0°45'	Low	259.05	35.184598	81.848897	1.67	5.58	109.65
17	Tennessee	132	1967	E rail	0°45'	High	259.05	35.184403	81.849000	1.03	10.73	37.30
18	Tennessee	132	1967	D rail	0°45'	High	259.05	35.184073	81.849182	2.58	9.30	74.25
19	Tennessee	132	1967	B rail	0°45'	Right	T259.26	35.183561	81.849471	0.81	11.67	8.13
20	Tennessee	132	1959	F rail	0°0'	Left	T259.26	35.183410	81.849490	2.06	5.94	141.41
21	Tennessee	132	1959	B rail	0°0'	Left	T259.26	35.183245	81.849580	3.33	8.18	120.63
22	Tennessee	132	1959	CC	1°45'	Low	259.58	35.176725	81.852775			211.30
23	Tennessee	132	1959	CC	1°45'	Low	259.58	35.176527	81.852918	2.02	6.87	188.48
24	Tennessee	132	1959	CC	1°45'	Low	259.58	35.176087	81.853217	2.96	0.66	132.87
25	Tennessee	132	1959	CC	1°45'	Low	259.58	35.175980	81.853297	1.11	10.53	119.60
26	Tennessee	132	1959	CC	1°45'	Low	259.58	35.175881	81.853371	2.05	9.58	107.02
27	Tennessee	132	1960	CC	2°0'	Low	266.92	35.071603	81.863853	2.70	9.06	4.95
28	Tennessee	132	1960	CC	2°0'	Low	266.92	35.071237	81.863735	10.36	1.40	47.88
29	Tennessee	132	1960	CC	2°0'	Low	266.92	35.070772	81.863550	4.60	7.04	100.78
30	Tennessee	132	1960	CC	2°0'	Low	266.92	35.070211	81.863307	0.50	11.26	166.60
31	Tennessee	132	1960	CC	1°15'	Low	265.59	35.093580	81.867782	3.16	8.35	4.41
32	Tennessee	132	1960	CC	1°15'	Low	265.59	35.093305	81.867773	7.97	1.03	34.74
33	Tennessee	132	1960	CC	1°15'	Low	265.59	35.092850	81.867728	1.90	9.61	83.70
34	Beth Steelton	132	1979	CC	1°15'	Low	265.59	35.092508	81.867715	3.64	1.37	120.46

B.2 NRC Sectioned CSX rail samples

A number of the CSX rail samples listed in Section B.1 were sectioned either using a water jet cutter or milling system. Summaries of photographs and measured crack lengths and depths are given in the several figures of this section.

CSX Blue Ridge Subdivision Sample #2



MP 224.45 LOW
Rail Manufacturer: Nippon
Rail Year: 1996
Rail Type: VT
Rail Weight: N/A

Measured crack depth

MRX: 0.1
Rohmann: 2.1-2.3

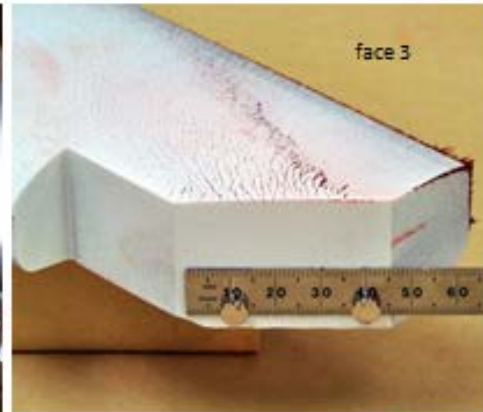
Magnetic Particle Inspection

	Face 2	Face 3
Max Length (mm)	1.6	1.2
Crack Angle (deg)	32	87
Max Depth (mm)	0.9	1.16
Surface Angle (deg)	82	35

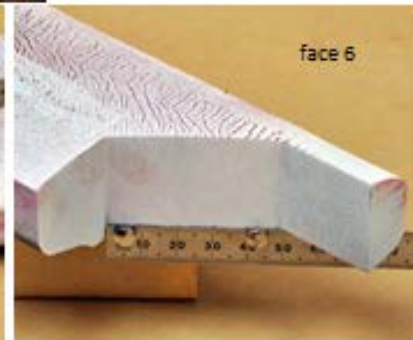
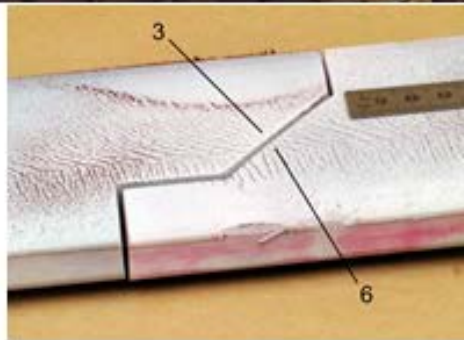
Figure 17: CSX Rail sample #2. Water jet cut perpendicular to surface cracks.

CSX Blue Ridge Subdivision Sample #4

MP 224.45 LOW
 Rail Manufacturer: Nippon
 Rail Year: 1996
 Rail Type: VT
 Rail Weight: N/A



Measured crack depth
 MRX: 0.1
 Rohmann: >5.0 mm



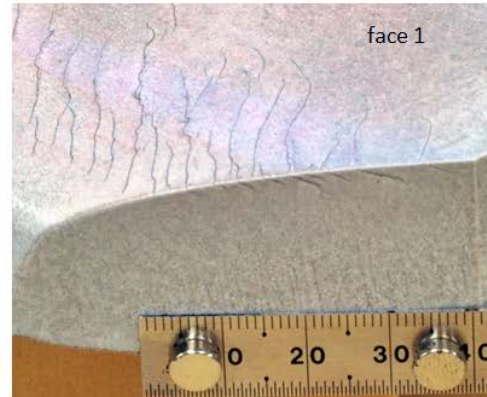
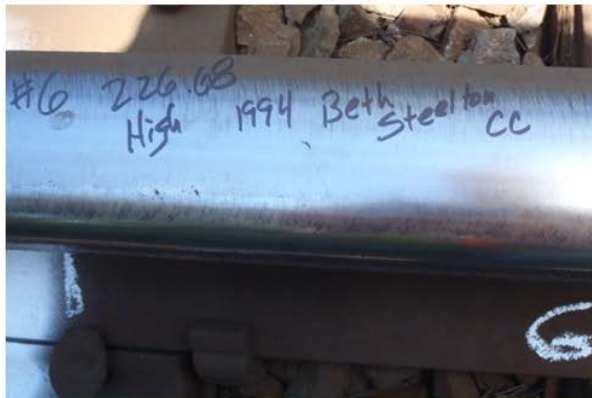
Magnetic Particle Inspection

	Face 3	Face 6
Max Length (mm)	1.2	1.0
Crack Angle (deg)	65	41
Max Depth (mm)	1.1	0.7
Surface Angle (deg)	49	49

Figure 18: CSX Rail sample #4. Water jet cut perpendicular to surface cracks with dry (red) magnetic particle enhancement of cracks.

CSX Blue Ridge Subdivision Sample #6

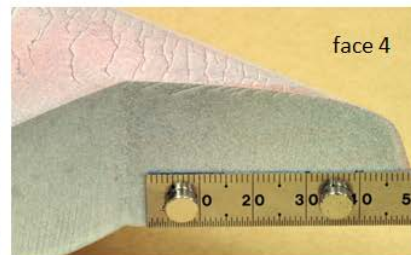
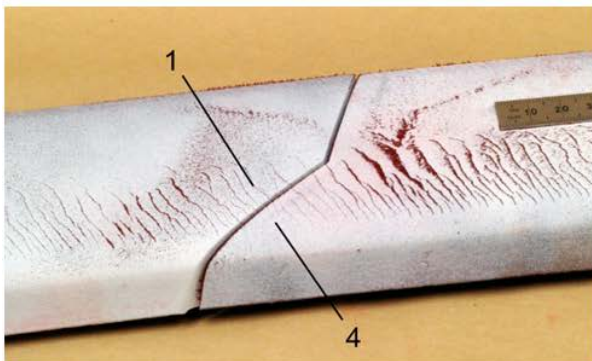
MP 226.68 HIGH
 Rail Manufacturer: Beth Steelton
 Rail Year: 1994
 Rail Type: CC
 Rail Weight: 136-10



Measured crack depth

MRX: 4.3

Rohmann: 3.1-3.8



Magnetic Particle Inspection

	Face 1	Face 4
Max Length (mm)	4.9	5.9
Crack Angle (deg)	23	23
Max Depth (mm)	1.9	2.3
Surface Angle (deg)	65	65
+Longitudinal cuts		

Figure 19: CSX Rail sample #6. Water jet cut perpendicular to surface cracks with dry and liquid magnetic particle enhancement.

CSX Blue Ridge Subdivision Sample #6

MP 226.68 HIGH
 Rail Manufacturer: Beth Steelton
 Rail Year: 1994
 Rail Type: CC
 Rail Weight: 136-10



Measured crack depth

MRX: 4.3
 Rohmann: 3.1-3.8

Magnetic Particle Inspection

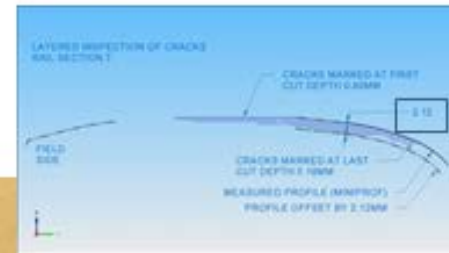
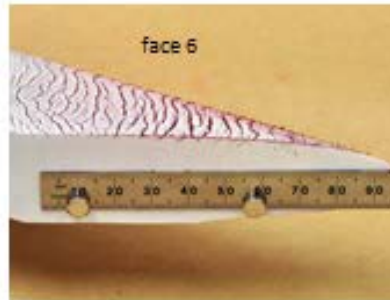
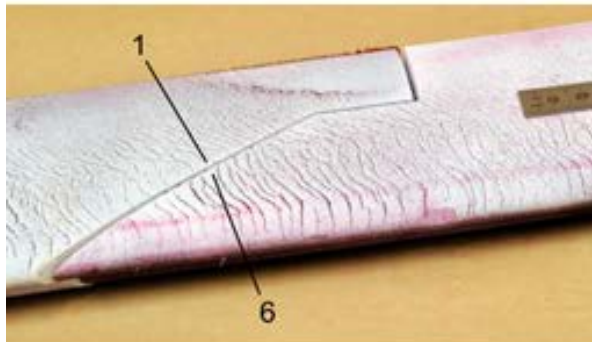
	Face 4	Face 3
Max Length (mm)	3.5	4.96
Crack Angle (deg)	32.8	23.5
Max Depth (mm)	2.10	2.21
Surface Angle (deg)		

Figure 20: CSX Rail sample #6. Water jet cut along the length of the rail, liquid magnetic particle enhancement.

CSX Blue Ridge Subdivision Sample #7

MP 240.21 HIGH
 Rail Manufacturer: Beth Steelton
 Rail Year: 1996
 Rail Type: CC
 Rail Weight: 136-10

Measured crack depth
 MRX: 6.3
 Rohmann: >5.0



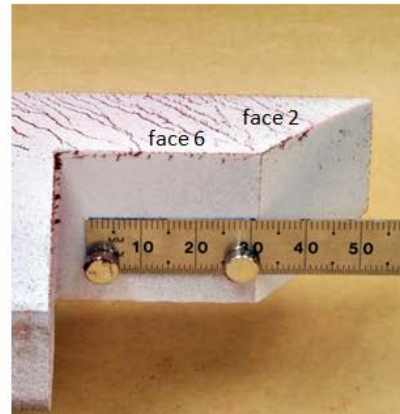
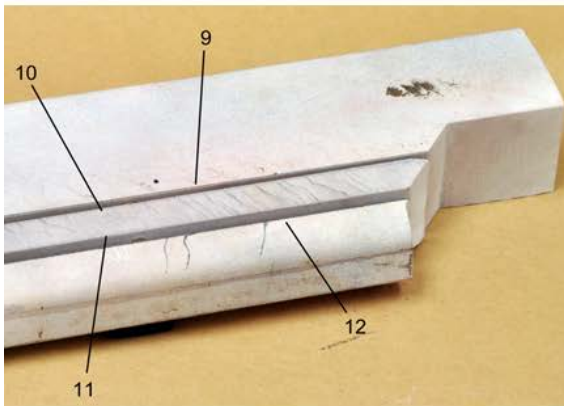
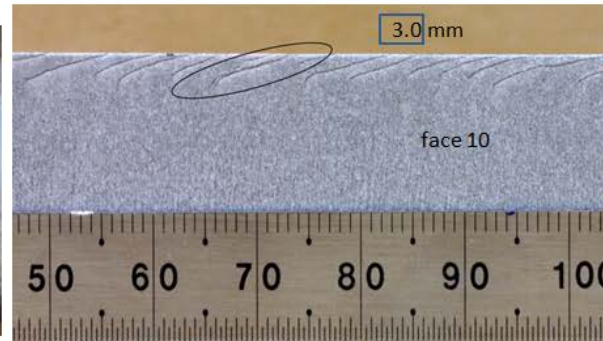
Magnetic Particle Inspection

	Face 1	Face 6
Max Length (mm)	2.8	4.2
Crack Angle (deg)	26	29
Max Depth (mm)	1.2	2.04
Surface Angle (deg)	63	63

Figure 21: CSX Rail sample #7. Water jet cut perpendicular to surface cracks, dry (red) magnetic particle enhancement of cracks. And then milled down through top of rail in 0.4 mm increments.

CSX Blue Ridge Subdivision Sample #12

MP T247.79 RIGHT
 Rail Manufacturer: Tennessee
 Rail Year: 1975
 Rail Type: CC
 Rail Weight: 132



Measured crack depth

MRX: 6.9
 Rohmann: >5.0

Magnetic Particle Inspection

	Face 2	Face 6
Max Length (mm)	3.8	2.0
Crack Angle (deg)	23	75
Max Depth (mm)	1.5	2.0
Surface Angle (deg)	46	46

Figure 22: CSX Rail sample #12. Water jet cut perpendicular to surface cracks, and then along the length of the rail, dry (red) and liquid magnetic particle enhancement.

CSX Blue Ridge Subdivision Sample #14



Measured crack depth

MRX: 4.8

Rohmann: 2.0–5.0

MP C259.05 High

Rail Manufacturer: Tennessee

Rail Year: 1967

Rail Type: E rail

Rail Weight: 132

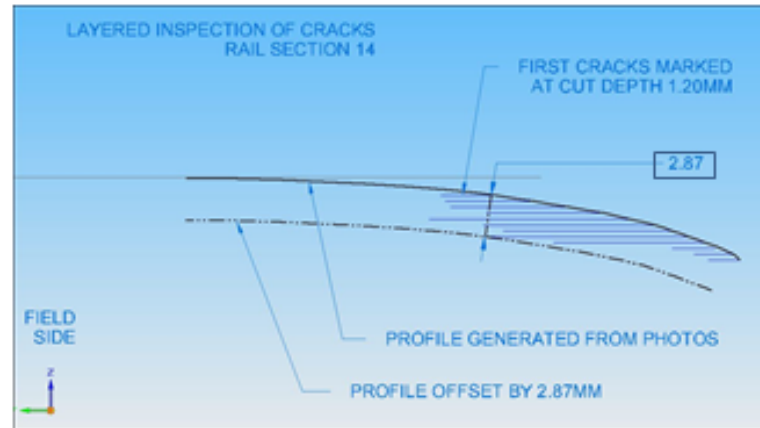
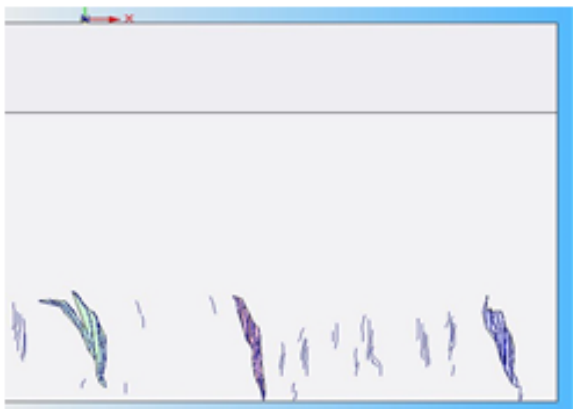
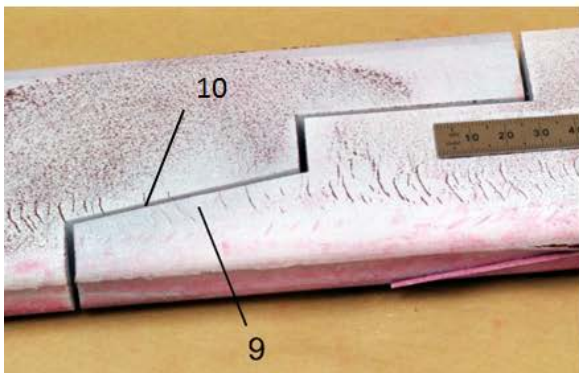
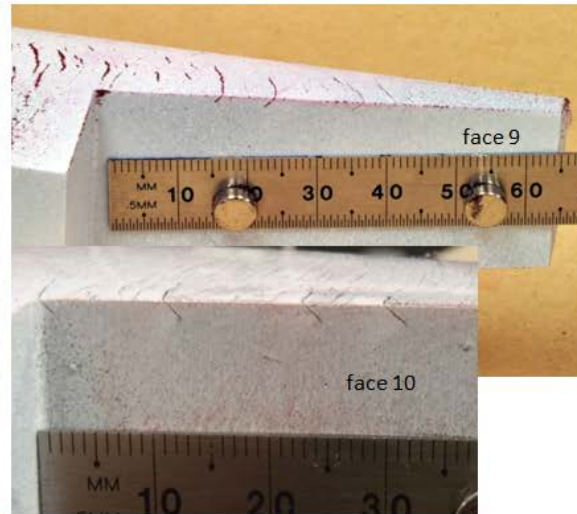


Figure 23: CSX Rail sample #14. Milled through the rail crown in 0.4 mm increments.

CSX Blue Ridge Subdivision Sample #16

MP 259.05 LOW
 Rail Manufacturer: Tennessee
 Rail Year: 1957
 Rail Type: C Rail
 Rail Weight: 132



Magnetic Particle Inspection

	Face 9	Face 10
Max Length (mm)	2.0	2.43
Crack Angle (deg)	48	43
Max Depth (mm)	1.5	1.48
Surface Angle (deg)	77	

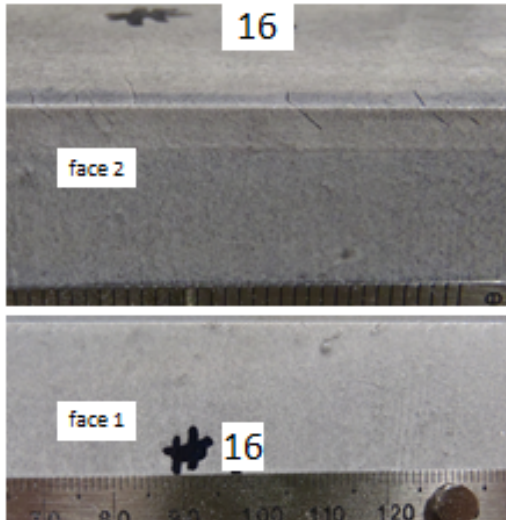
Measured crack depth

MRX: 2.1
 Rohmann: none

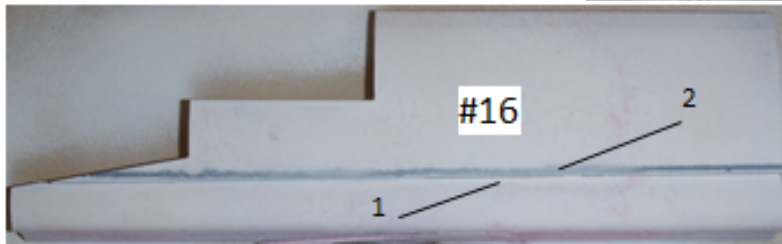
Figure 24: CSX Rail sample #16. Water jet cut perpendicular to surface cracks, dry (red) magnetic particle enhancement.

CSX Blue Ridge Subdivision Sample #16

MP 238.3 Low
 Rail Manufacturer: Beth Steelton
 Rail Year: 1996
 Rail Type: CC
 Rail Weight: 136-10



Measured crack depth
 MRX: 2.1
 Rohmann: none

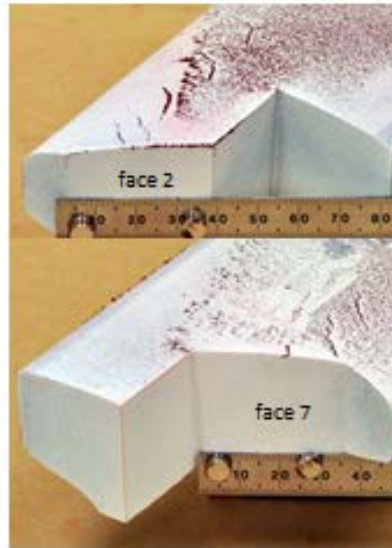
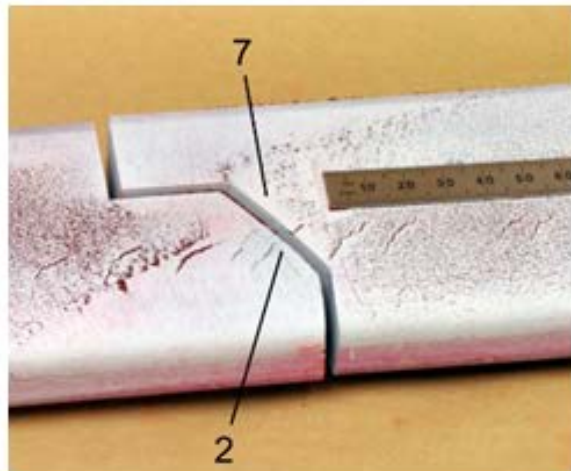


Magnetic Particle Inspection

	Face 1	Face 2
Max Length (mm)	2.25	2.08
Crack Angle (deg)	42	46
Max Depth (mm)	1.65	1.52
Surface Angle (deg)	77	

Figure 25: CSX Rail sample #16. Water jet cut along the length of the rail, liquid magnetic particle enhancement.

CSX Blue Ridge Subdivision Sample #18



MP 259.05 HIGH
 Rail Manufacturer: Tennessee
 Rail Year: 1967
 Rail Type: D Rail
 Rail Weight: 132

Measured crack depth

MRX: 1.3
 Rohmann: none

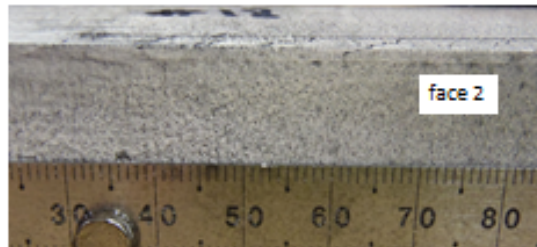
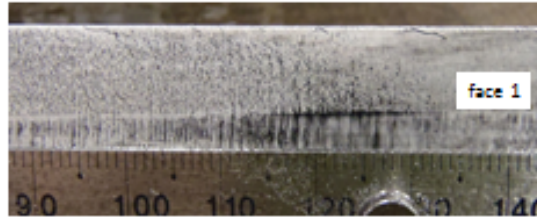
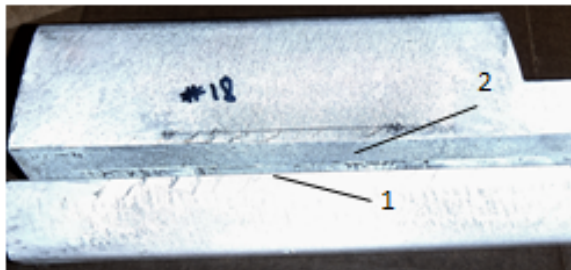
Magnetic Particle Inspection

	Face 2	Face 7
Max Length (mm)	2.5	1.3
Crack Angle (deg)	20	28
Max Depth (mm)	0.8	0.6
Surface Angle (deg)	48	48

Figure 26: CSX Rail sample #6. Water jet cut along the length of the rail, liquid magnetic particle enhancement.

CSX Blue Ridge Subdivision Sample #18

MP 259.05 HIGH
 Rail Manufacturer: Tennessee
 Rail Year: 1967
 Rail Type: D Rail
 Rail Weight: 132



Magnetic Particle Inspection

	face 1	face 2
Max Length (mm)	3	3.96
Crack Angle (deg)	13	20
Max Depth (mm)	0.9	1.20
Surface Angle (deg)	48	48

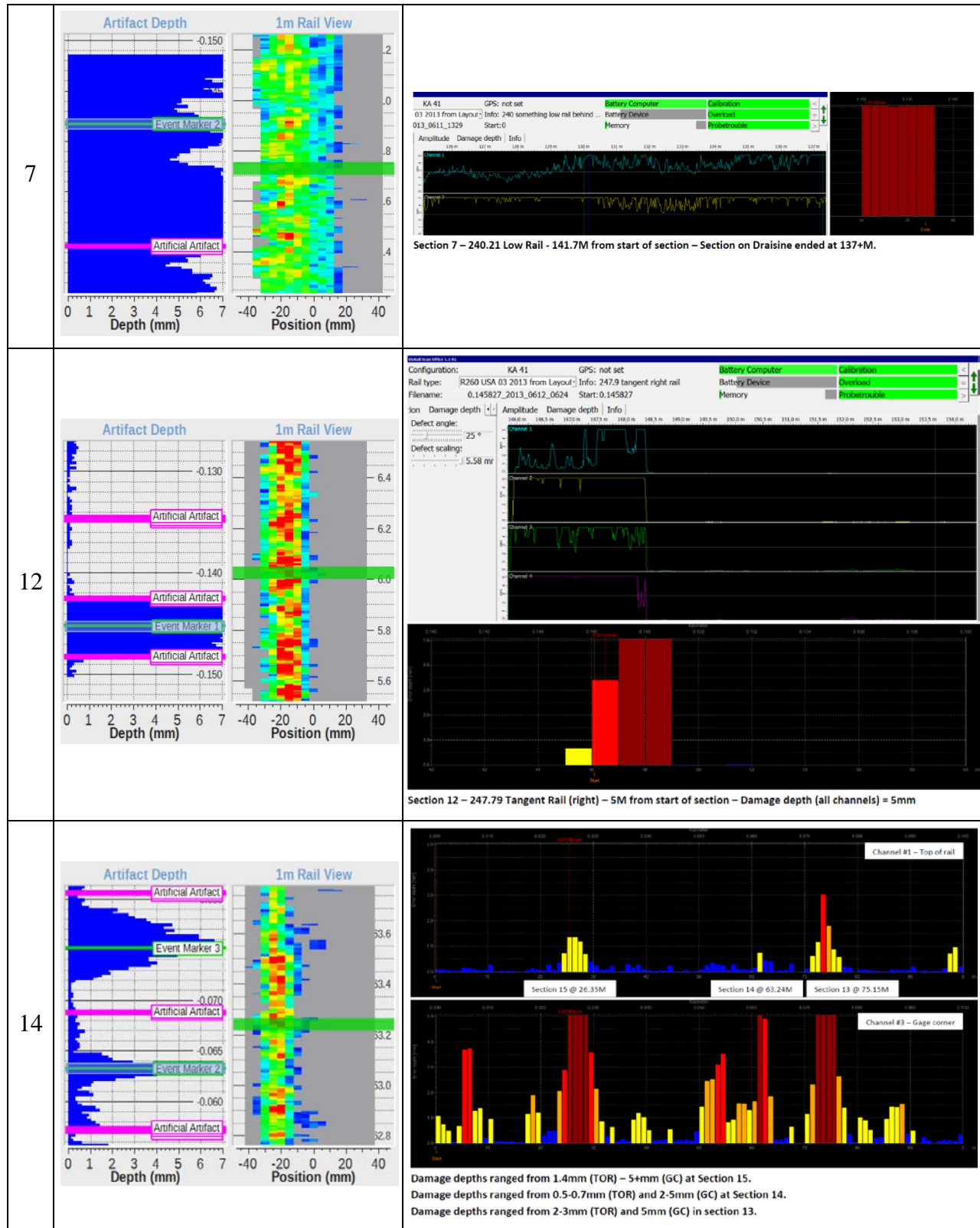
Measured crack depth

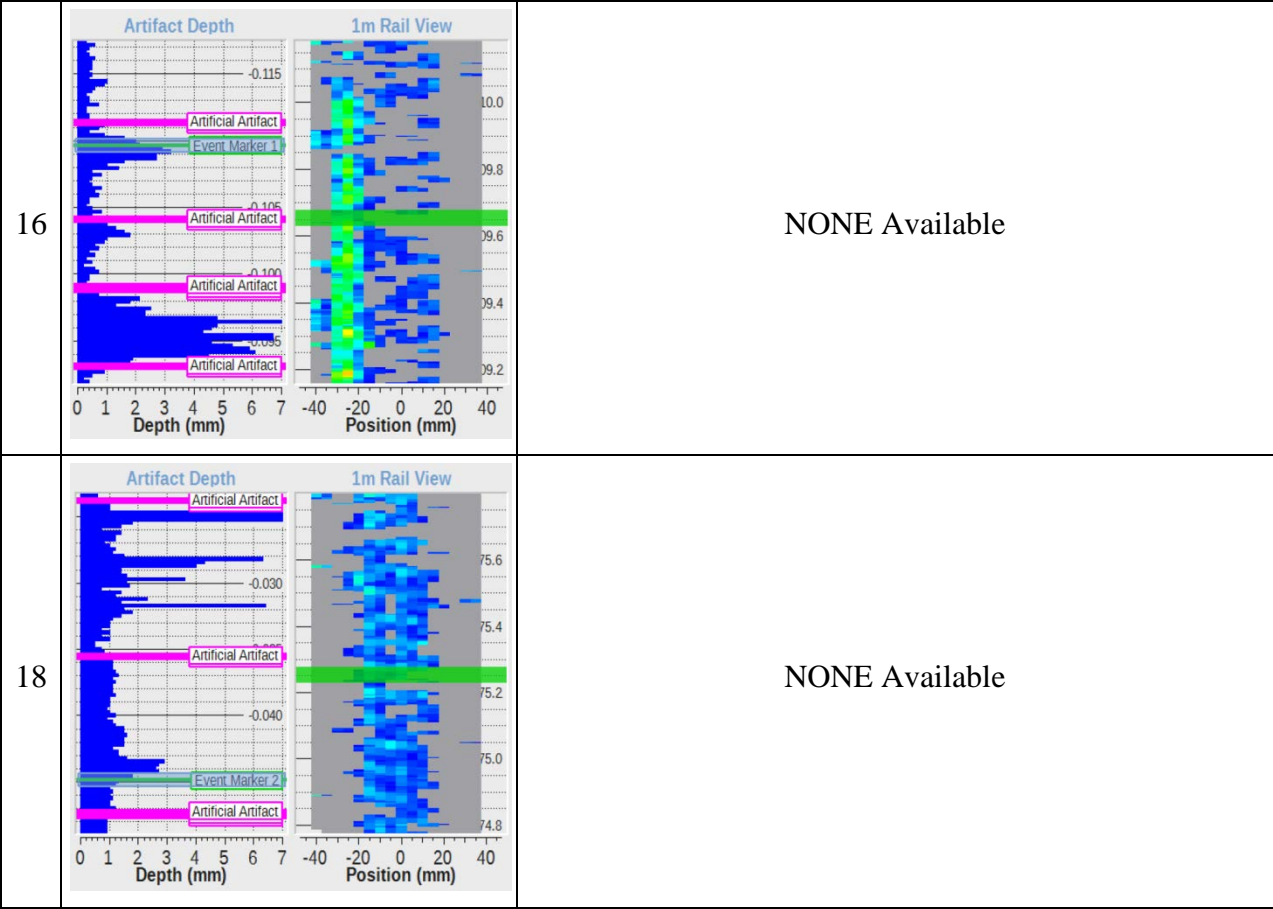
MRX: 1.3
 Rohmann: none

Figure 27: CSX Rail sample #18. Water jet cut along the length of the rail, liquid magnetic particle enhancement.

B.2.1. Non-Destructive Testing (NDT) crack measurements of CSX rail samples

#	RSCM	Rohmann
2		<p>Section 2 – 224.45 Low Rail - 75.87M from start of Section – Damage Depth Channel 1 = 2.1-2.3mm</p>
4		<p>Section 4 – 224.45 Low Rail – 151M from start of section – Damage Depth Channel 1 = 5mm (or greater)</p>
6		<p>Section 6 – 226.68 High Rail – 55.2M from start of section – Damage Depth channel 4 = 3.1-3.8mm (Ch 3 = 5+mm)</p>





B.3 NS Railways samples from February 2014

B.3.1. NS metallurgical sectioning



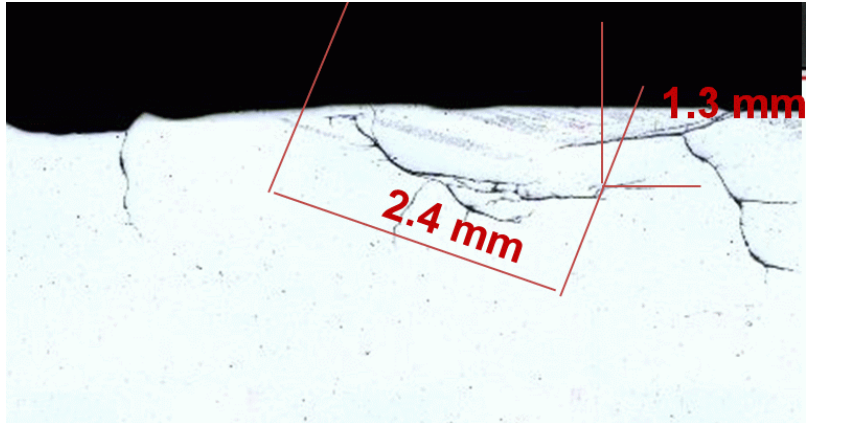
 A photograph of a rail's surface. The top half shows a dark, textured surface with some white markings, including the number '4' and '2343'. The bottom half shows a bright, orange-red, elongated crack or defect.		Surface condition
 A photograph of a rail's cross-section. The top edge is dark and rough, while the interior is a lighter, more uniform color. A horizontal line is visible across the middle.		Cross section
 A photograph of a rail's cross-section with a crack. Red lines and text indicate measurements: '1.3 mm' for the crack's width and '2.4 mm' for its length.		Crack measurement

Figure 28: NS Labs analysis of Sample 4



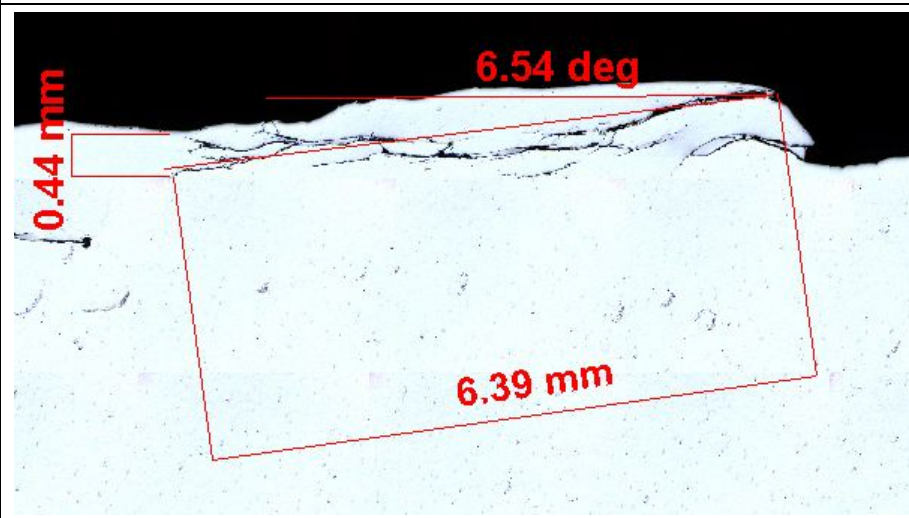
 <p>A close-up photograph of the surface of Sample 5. The surface is light-colored and shows numerous small, dark, irregular spots and pits, indicating surface degradation or corrosion. Handwritten markings in black ink are visible in the upper left corner, including the number '6' and some illegible characters.</p>		Surface condition
 <p>A photograph showing a cross-section of Sample 5. The material appears dark and granular, with a rough, uneven surface. The cross-section reveals internal texture and some surface irregularities.</p>		Cross section
 <p>A photograph showing a crack measurement on Sample 5. A red rectangular box highlights the crack area. The crack is labeled with a width of 0.44 mm and a length of 6.39 mm. The angle of the crack is labeled as 6.54 deg.</p>		Crack measurement

Figure 29: NS Labs analysis of Sample 5


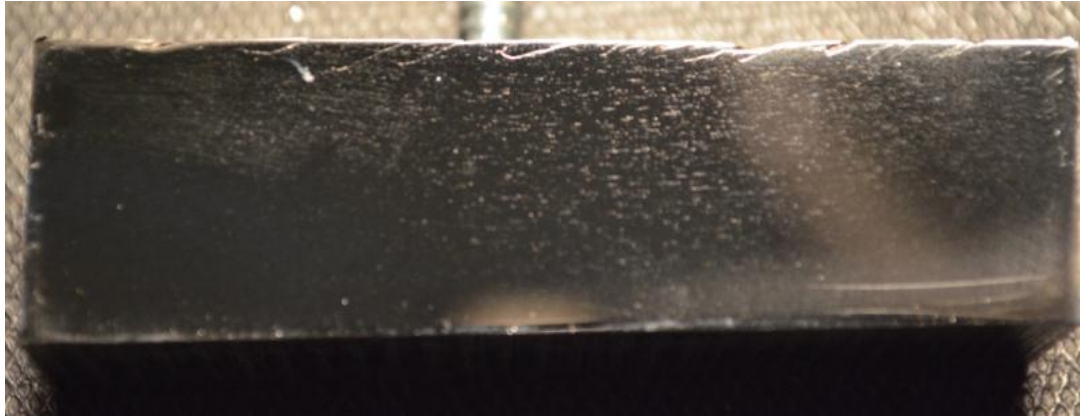
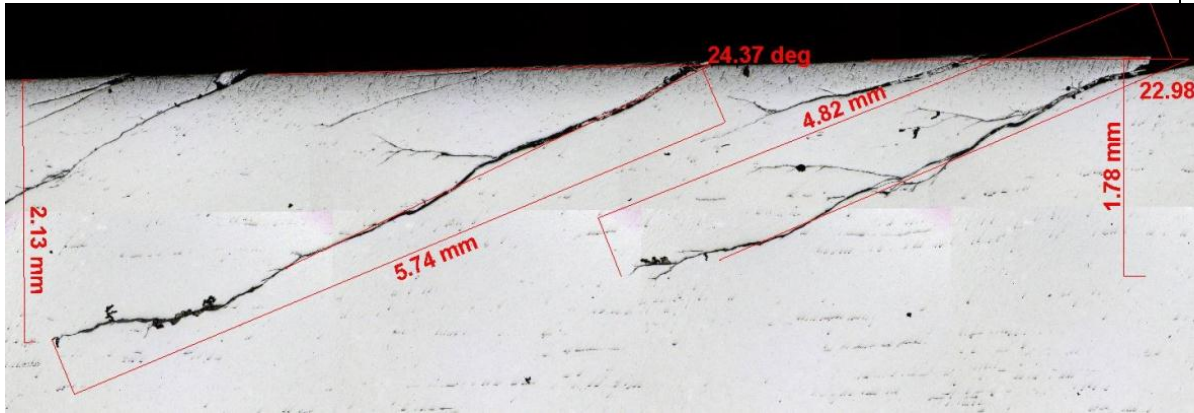
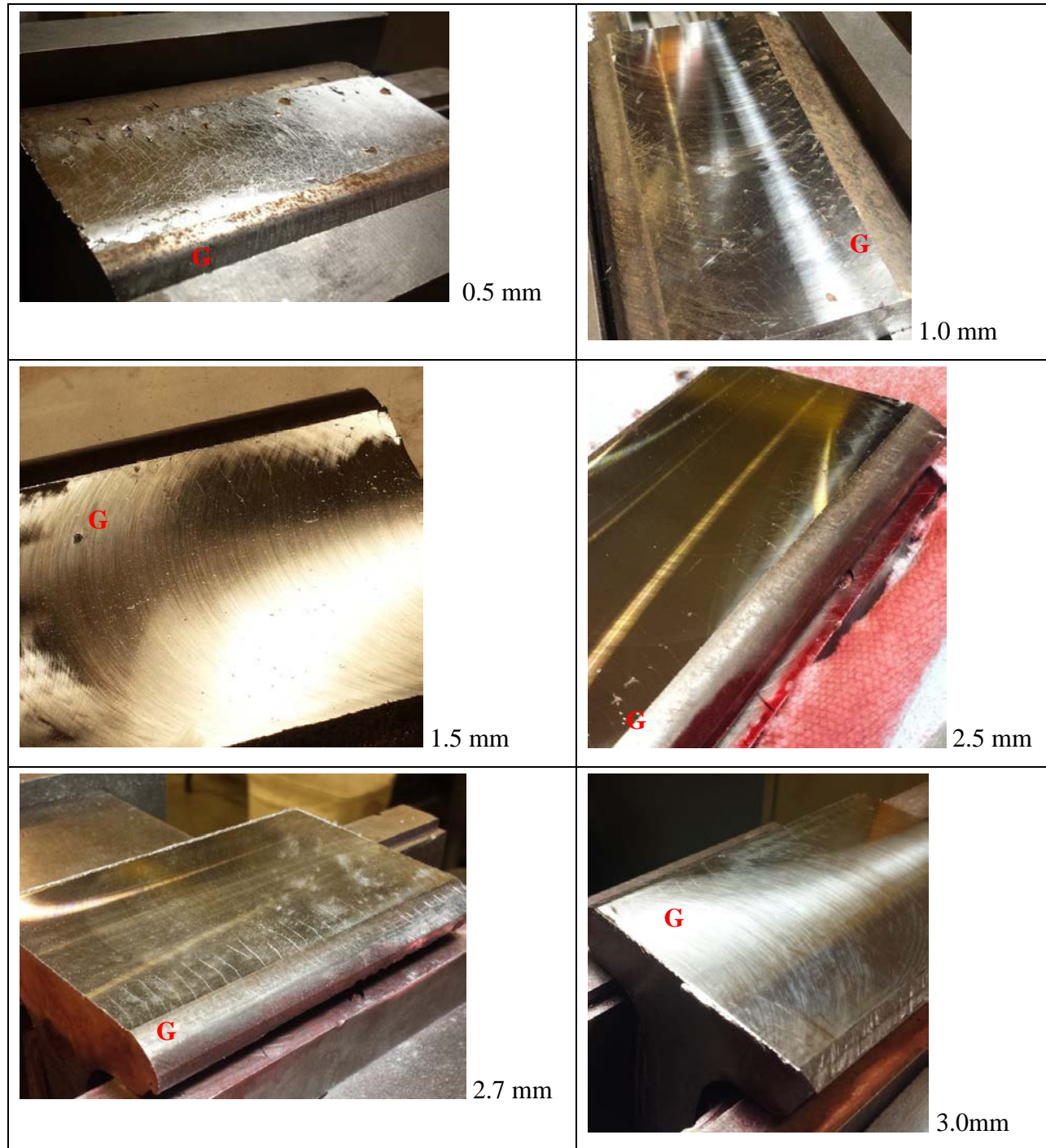
	Surface condition
	Longitudinal section
	Crack measurement

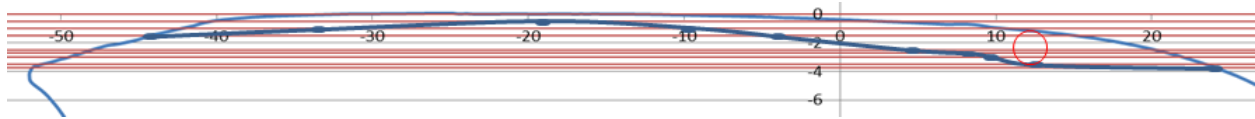
Figure 30: NS Labs analysis of Sample 6, longitudinal section

B.3.2. NS milling

Sample 5 from the NS Hardy Curve was milled at the NS laboratories. After each milling, a photograph of the surface was taken. These are shown below, labelled with the total depth of metal removed by milling. The gauge side of the rail is annotated with a 'G'.



Roughly estimating the width of the remaining crack band, and plotting that on the measured rail profile, allows the region of cracked material to be graphed. The circle has a diameter of about 2.3mm and represents the maximum depth of cracks for this sample.

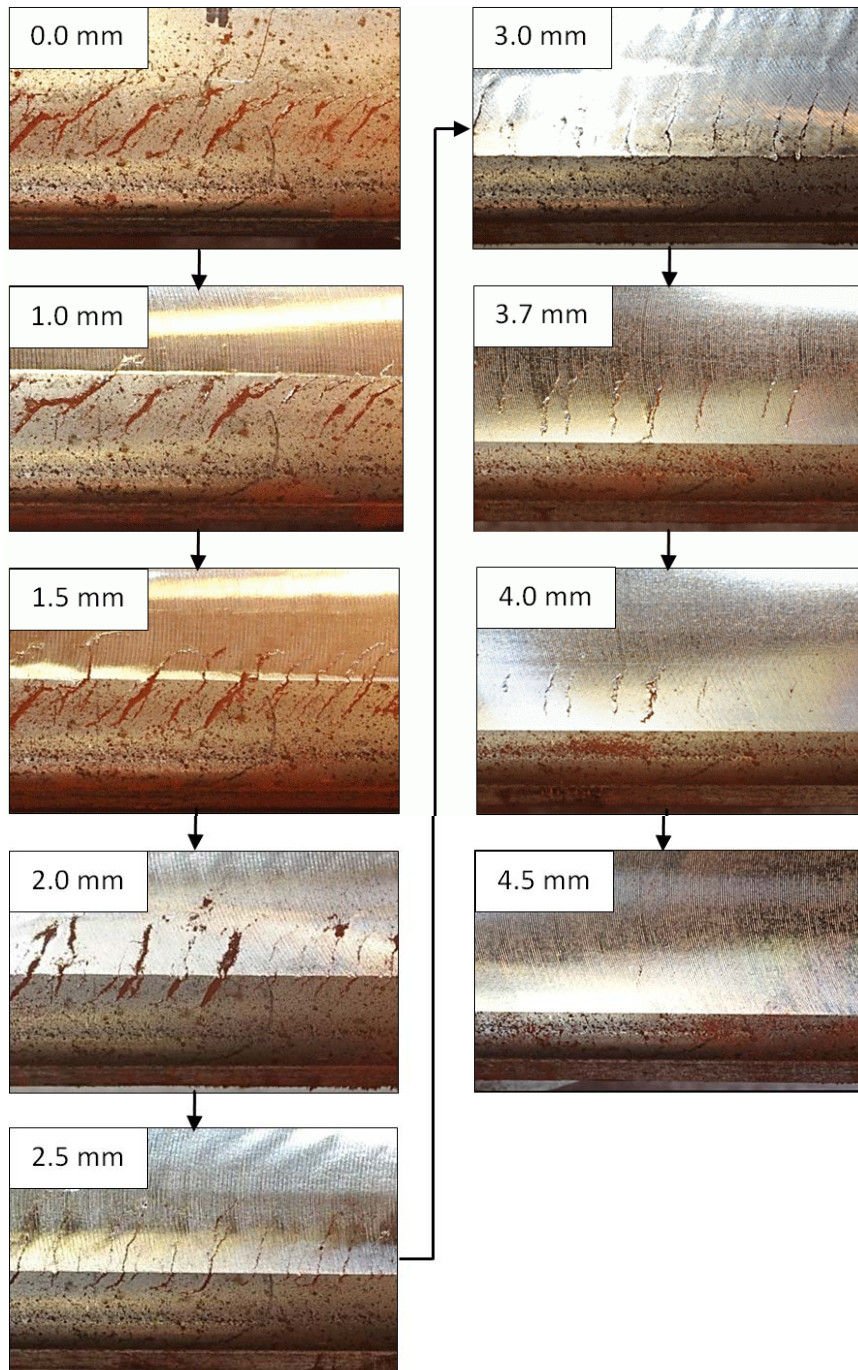


location	Main	sample #	metallurgy	coords	visual	sample length (cm)
MP 210.7	M1	1	132 US Illinois 1980	46-49'-33" N, 95-51'-32" W	moderate cracking	71.7
	M1	2	13225 USS Illinois 1972 I	46-49'-33" N, 95-51'-32" W	moderate cracking	72.8
	M1	3	13225 USS Illinois 1972 I		moderate cracking	76.7
MP 203.11 - 203.38	M1	4	132 CF&I 1982	46-44-52N, 95-45-14W	light cracking	106.5
	M1	5	13225 RE CC USS Illinois 1982	46-44-50N, 95-45-12W	light cracking	96.8
	M1	6	13225 RE CC USS Illinois 1981	46-44-48N, 95-45-9W	heavy cracking	107.4
MP 200.69		7	136 RMSM 2002	46-43-48 N, 95-42-21 W	heavy cracking, just ahead of crossing	63.3
		8	136RE VT		SSC - through crossing	45.5
		9	RMSM 2002		SSC - through crossing	47.4
	M2	10	2004?		very light cracking	69.0
		11	136-10 DR NKK 1994		very light cracking	63.1
MP200.4- 200.6	M2	12	141 2004 RMSM	46-43-40N, 95-42-6W	light cracking	97.7
	M2	13	136 Beth Steelton 1992	46-43-42N, 95-42-10W	VERY light cracking	111
Norfolk Southern		14			moderate cracking	49.3

B.4 BNSF Rail Samples from November 2014

B.4.1. Sample 3

Crack morphology between locations 11-14in.
Milling distance from top-of-rail is as indicated.
Gauge side of rail is on the bottom of each image.



B.4.2. Sample 4

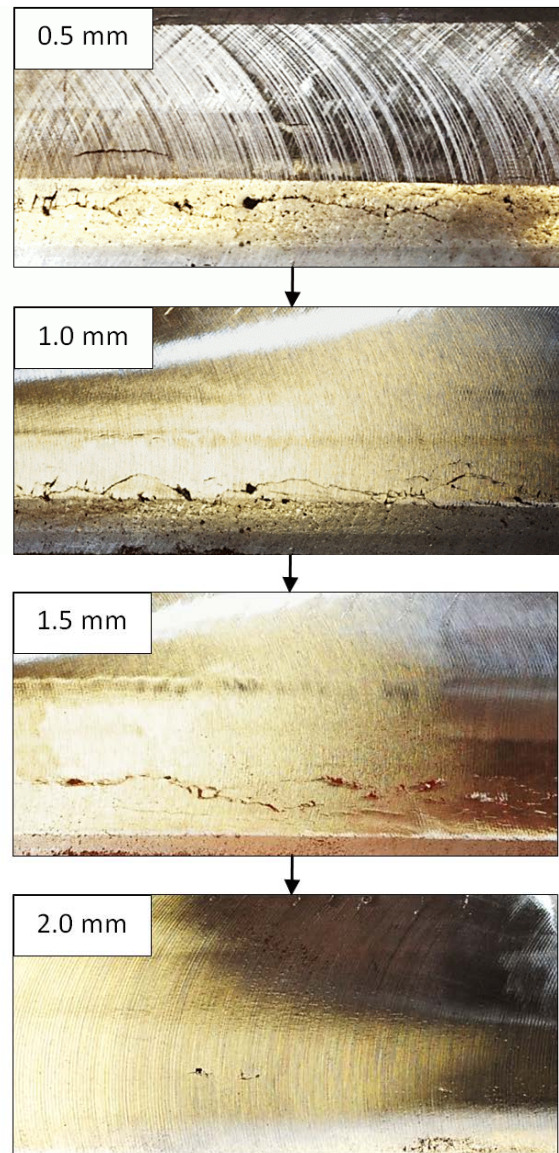
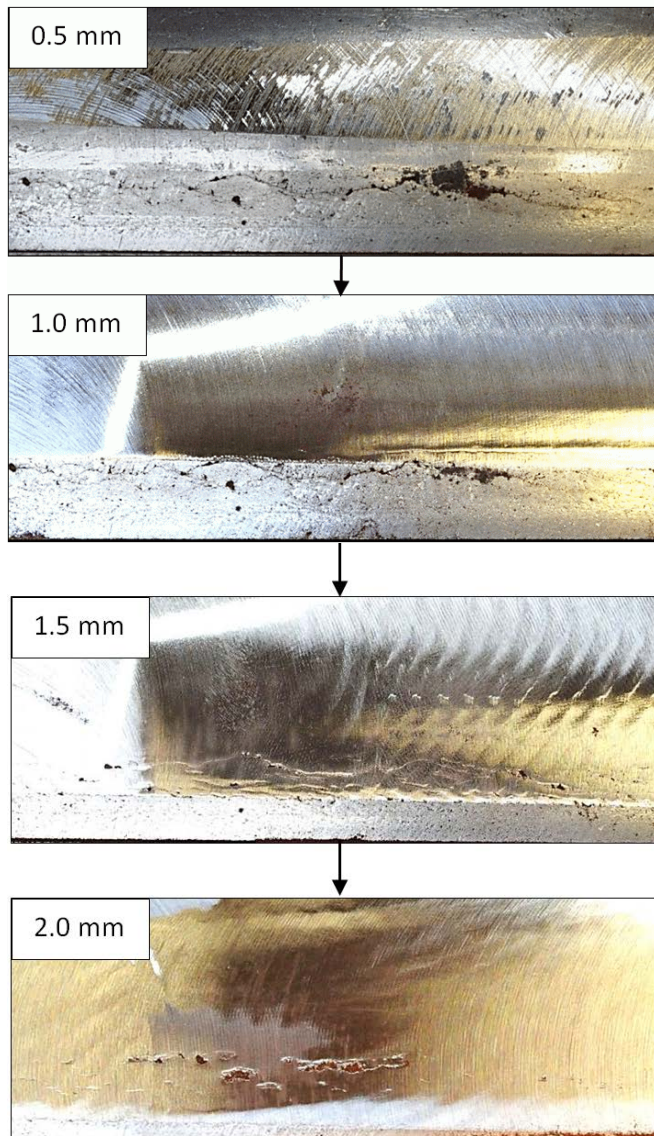
Left Side

Crack morphology between locations 18-23in.

Right Side

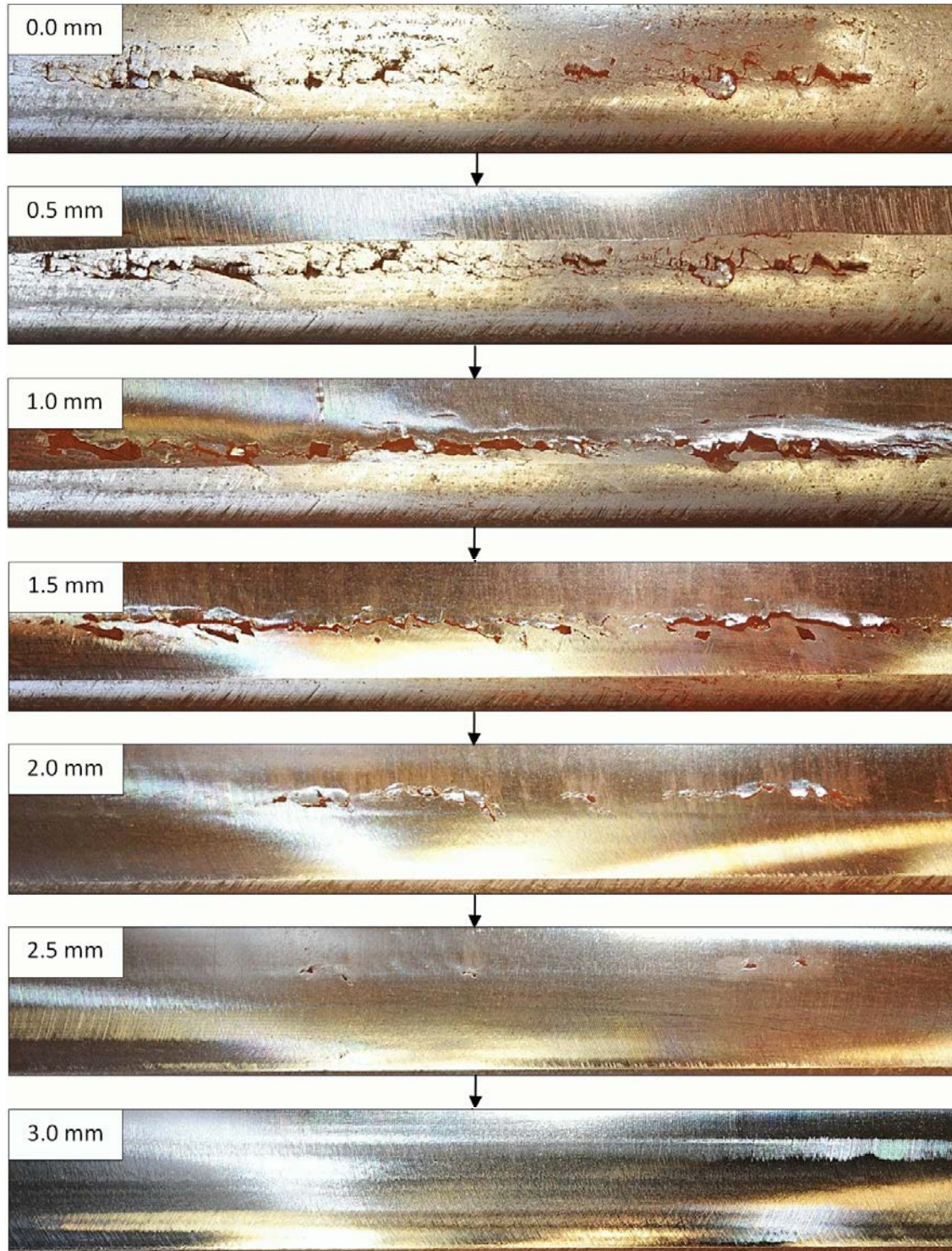
Crack morphology between locations 3-7in.

Milling distance from top-of-rail is as indicated.
Gauge side of rail is on the bottom of each image.



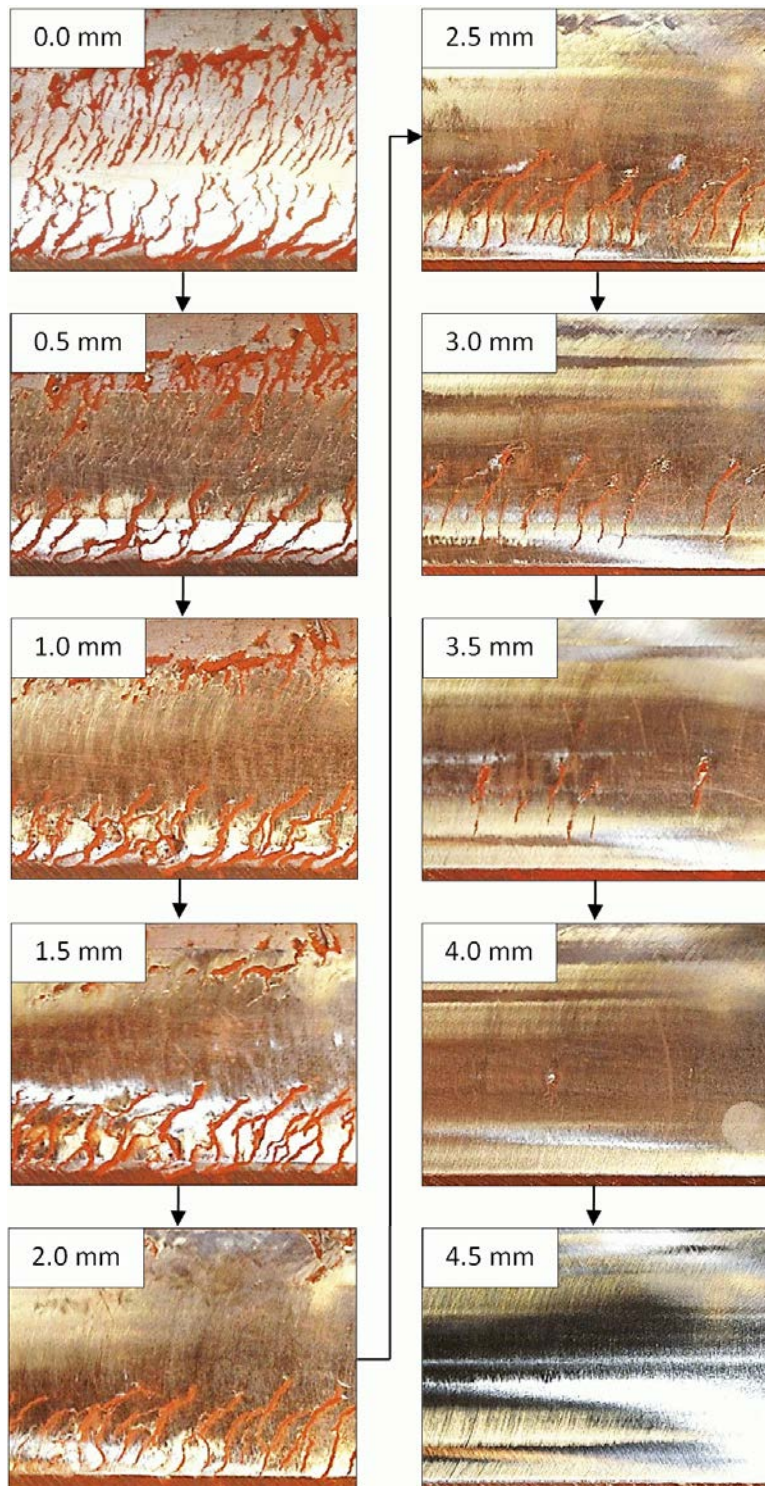
B.4.3. Sample 6

Crack morphology between locations 5-11 in.
Milling distance from top-of-rail is as indicated.
Gauge side of rail is on the bottom of each image.



B.4.4. Sample 8

Crack morphology between locations 8-11 in.
Milling distance from top-of-rail is as indicated.
Gauge side of rail is on the bottom of each image.

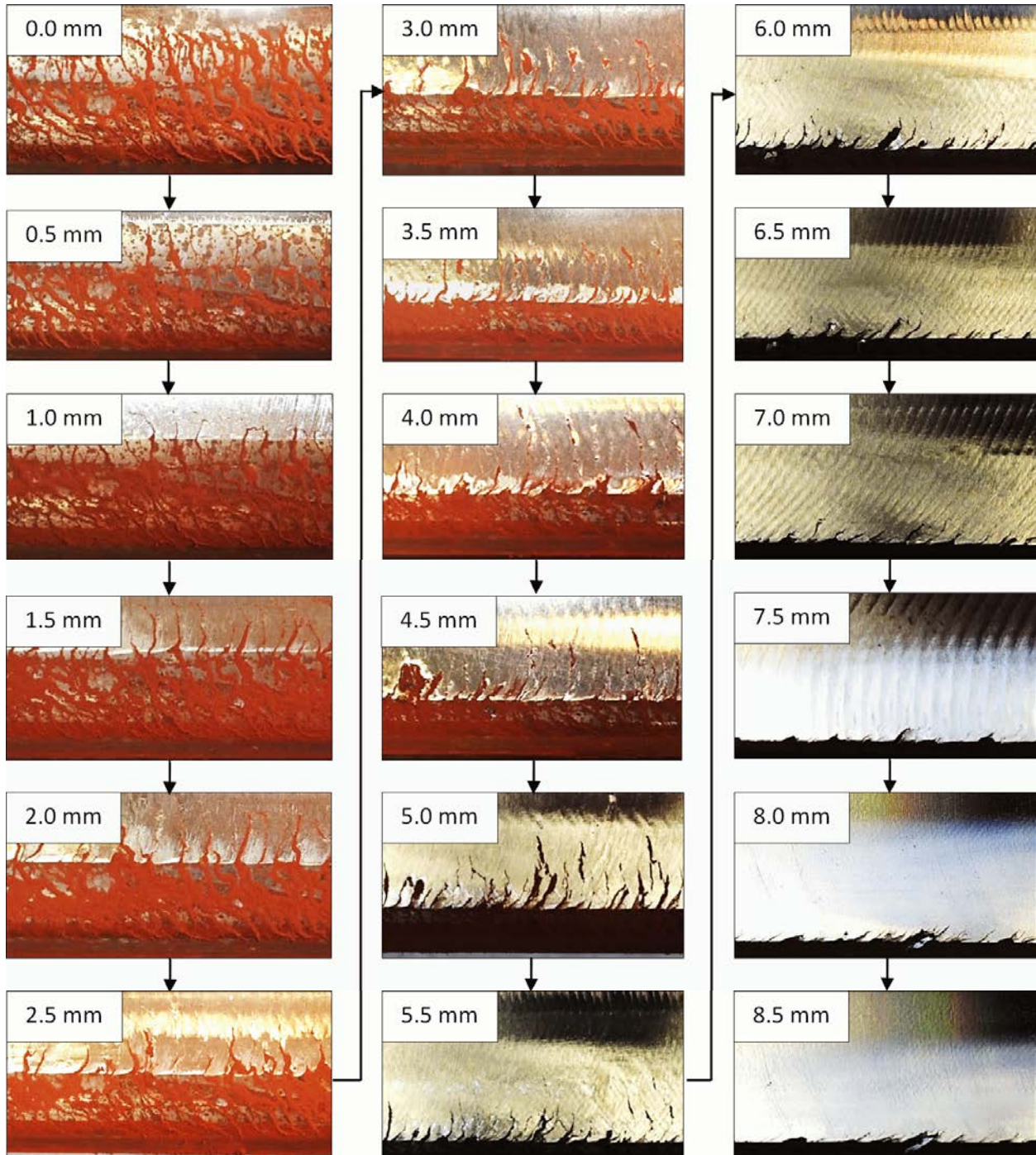


B.4.5. Sample 16

Crack morphology between locations 11-14in.

Milling distance from top-of-rail is as indicated.

Gauge side of rail is on the bottom of each image.



Abbreviations and Acronyms

BNSF	BNSF Railway
EDM	Electrical Discharge Machining
GQI	Grinding Quality Index
ICRI	International Collaborative Research Initiative
MGT	Million Gross Tons
NDT	Non-Destructive Testing
NRC	National Research Council, Canada
NS	Norfolk Southern Railways
RCF	Rolling Contact Fatigue
RSCM	Rail Surface Crack Measuring System